POLITECNICO DI MILANO

Scuola di Ingegneria Industriale e dell'Informazione

Corso di Laurea Magistrale in

Ingegneria Biomedica

Cardiac rhythm classification and mortality risk assessment from RR intervals using non-linear dynamics indexes

Relatore: Prof. Sergio Cerutti

Correlatore: Prof.ssa Manuela Ferrario

Dott. Joseph Randall Moorman

Tesi di Laurea di:

Luca Carozzi - Matricola 787464

Marta Carrara - Matricola 784390

Anno Accademico 2012-2013

Acknowledgments

We wish to thank our advisors, Prof. Sergio Cerutti, Prof.ssa Manuela Ferrario and Dott. J. Randall Moorman from the University of Virginia, for their guidance and for the passion they put in their job. Their fascinating interest and curiosity always drove us in the work of these months, which became, day after day, a great challenge to face.

We also would like to thank Douglas E. Lake, who was always present and ready to help, support and direct us with his tenaciousness and love for research.

We say thank to Gary, Katie, Patrick and Nick from the UVa team for their cheerfulness and friendship, which was very helpful and valuable.

A lot of gratitude is reserved to our families and relatives, who always support, believe and love us.

Finally, we say a big “thank you” to all the friends we met in these years of university, who accompanied us with love.

Contents

List of Acronyms:

ACC: American college of cardiologist

AF: atrial fibrillation

AFL: atrial flutter

AHA: American heart association

ANS: autonomic nervous system

AV node: atrioventricular node

COSEn: coefficient of sample entropy

DFA: detrended fluctuation analysis

ECG: electrocardiogram

ESC: European society of cardiology

HR: heart rate

HRV: heart rate variability

ICU: intensive care unit

k-NN: k-nearest neighbor

LD: local dynamics

LDs: local dynamics score

NSR: normal sinus rhythm

PACs: premature atrial contractions

PVCs: premature ventricular contractions

PPV: positive predictive value

QSE: quadratic sample entropy

SampEn: sample entropy

SA node: sinus atrial node

SD: standard deviation

SR: sinus rhythm

UVa: university of Virginia

Summary

Introduction

Cardiovascular diseases are the leading cause of death in most of the developed countries, being associated with more than 30% of all deaths (Go et al, 2013). Premature ventricular contractions (PVCs) lead to poor prognosis even in hearts with no structural diseases (Cha et al, 2012) (Lee et al, 2012). Premature atrial contractions (PACs) are known to precede atrial fibrillation (AF) (Haissaguerre et al, 1998) and to be a surrogate marker of paroxysmal AF in patients with acute ischemic stroke (Wallmann et al, 2007). AF is recognized to be one of the leading causes of stroke and a strong independent risk factor for increased cardiovascular morbidity and mortality (Benjamin et al, 1998) (Wolf et al, 1991) (Stewart et al, 2002), and it is very common among old subjects (Lake and Moorman, 2011). The world population is rapidly aging and this situation claims for an effective detection and monitoring of AF.

Important clinical decisions are related to the presence of AF, including stroke prevention with anticoagulants or left atrial appendage exclusion, cardioversion, ablation, and antiarrhythmic drugs. On contrast, no treatments are required even in situations with high burden of PVCs or PACs without concomitant pathological conditions, such as cardiomyopathy.

Current devices for arrhythmias detection, such as ECG Holter recordings, are obtrusive for the patient and are based on ECG signal, which can be distorted and noisy, making features extraction from the waveform not always feasible.

The RR interval time series is a reliable signal, it requires less computational cost and it’s less affected by high frequency noise.

However, non-invasive devices for determining heart rhythm are not commonly used because of reduced confidence in detecting AF based only on the heart rate or RR series. In fact, many methods to distinguish between AF and Normal Sinus Rhythm (NSR) has been proposed, given the largely different dynamics

between the two rhythms (Sarkar et al, 2008) (DeMazumder et al, 2013) (Lake and Moorman, 2011) (Tateno and Glass, 2001), but situations of sinus rhythm (SR) with frequent ectopy, atrial or ventricular, is expected to share features with AF, and thus to be distinguished with difficulty.

The principal objective of this thesis is to provide an algorithm for the detection and classification of AF even when a very high burden of atrial and ventricular ectopic beats is present, based only on RR intervals time series. We hypothesized that indices related to the dynamics of RR series can contribute to a better distinction of SR with ectopy from AF. We tested the hypothesis using three nonlinear indices. The Coefficient of Sample Entropy (COSEn) was designated to quantify the higher entropy characteristics of AF with respect to NSR, and the algorithm was optimized for very short time series (Lake and Moorman, 2011). Local Dynamics score (LDs) is a new index proposed to capture local dynamics of the heart rate, that are related to the baseline variability and to the outliers, such as ectopy (Moss et al, 2014), and it was also designed to work on 12-beat segments. Detrended Fluctuation Analysis (DFA) is a well-known method to quantify the fractal-like scaling properties of the RR interval time series (Peng et al, 1995).

The second objective was to analyze the mortality risk over 2 years of the same population, based on COSEn and LDs indices only. We hypothesized that the combination of these two entropy-based dynamical measures could help to shed light on association between cardiac arrhythmias and mortality risk.

Material and Methods

We studied RR interval time series from 24 hour Holter recordings collected from 2’722 consecutive patients at the University of Virginia (UVa) Heart Station from 12/2004 to 10/2010. The RR series were subdivided into 377’285 10-minute segments. Each 10-minute segment was classified as AF if the burden of AF was greater than 5%, as SR with ectopy if the burden of ectopy was more than 10%, as NSR otherwise. Thus, the dataset is composed of 79% NSR, 8% AF and 13% SR with ectopy segments. The 3 categories are mutually exclusive and reflect clinical practice.

To test the overall hypothesis that dynamical measures were useful for rhythm classification, we used several schemes. The strategy was to compare the accuracy of classification using means and standard deviations of RR series alone, and after addition of the 3 dynamical measures - COSEn, LDs and slope of DFA. The first scheme was a system of 3 multivariate logistic regression models, each used to distinguish one rhythm class from the other two. The second approach was a k-nearest neighbors technique. All models were validated using a 10-fold cross-validation procedure on the entire dataset. Finally, the models were externally validated on the MIT-BIH database.

We assessed mean, standard deviation, COSEn and LDs on 30 second segments and then we averaged the results over 10 minute, while DFA was computed on 10-minute segments.

As regard the analysis of the mortality risk, we performed a multivariate kernel density study on the histograms of the joint distributions of COSEn and LDs estimated on the UVa database. The kernel chosen is a bivariate Gaussian with a diagonal bandwidth matrix, which allows different amounts of smoothing in each of the coordinates (Botev et al, 2010). The two bandwidth parameters are chosen optimally without assuming a parametric model for the data (Lake, 2009).

Results

Our major finding is the improvement in the distinction of SR with ectopy using the dynamical measures from the other two groups. The positive predictive value using either regression models or k-nearest neighbor (*k*-NN) analysis was 85%, with higher values for the diagnosis of NSR (96%) and AF (90%). The accuracy increased further if the threshold for diagnosing ectopy was higher than 10% burden.

Surprisingly, these measures do not distinguish well between atrial and ventricular premature beats, a potentially important clinical distinction. PACs may be harbingers of AF, and PVCs are associated with increased mortality, especially when structural heart disease is present. We tested a logistic regression scheme with 4 models to distinguish among NSR, AF, SR with PVCs and SR with PACs but a large misclassification error occurred when the two ectopy classes are separately analyzed.

The models were externally validated using the canonical MIT-BIH databases of NSR, AF and other arrhythmias (ARH). Here the positive predictive values for NSR and AF rose to 99% and 96%, respectively, but fell for SR with ectopy to 45%. This may be explained by the much lower incidence of SR with ectopy in the highly selected MIT-BIH databases, where they represented <1% of the 11'196 10-minute segments, compared with 13% of the 377'825 10-minute segments in the UVa database.

The second objective was to analyze the mortality risk over 2 years of the population considering only patients with age over 40 years. The result is a color map of the risk, shown in Figure 1.

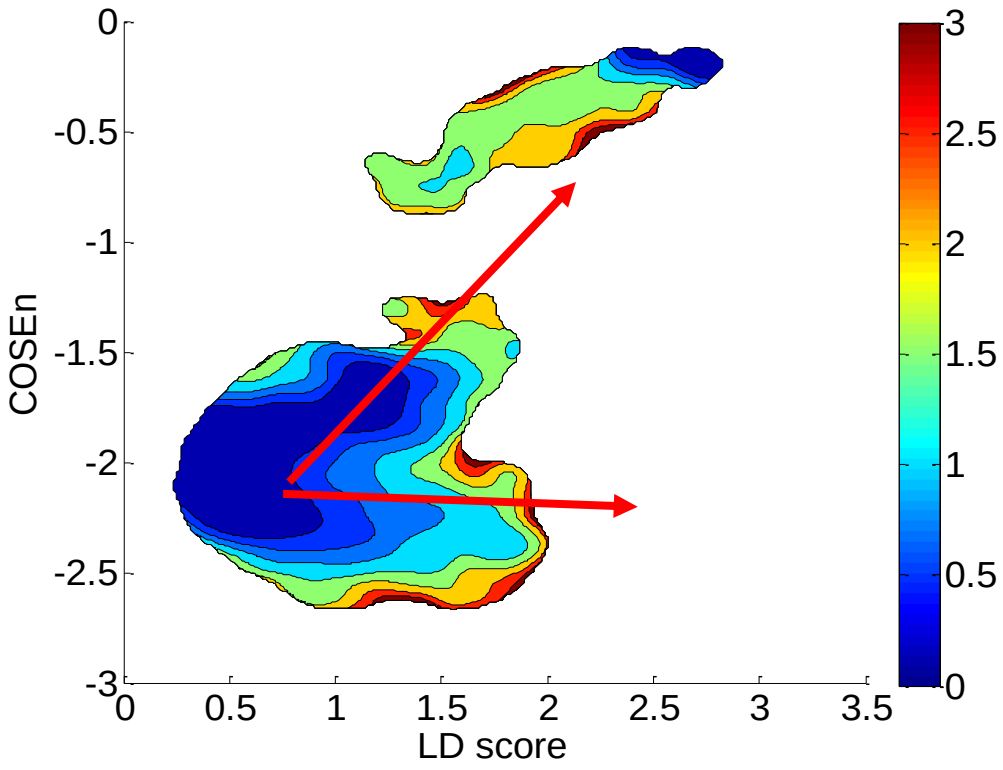

Figure 1. Mortality risk over 2 years of the UVa Holter population

A well-defined royal blue region, i.e. with very low mortality risk, is characterized by low values of LDs, whereas high-risk zones are related to higher values of the index. In particular, starting from the low risk region (left lower edge), it is possible to distinguish two different directions along which the risk becomes higher: the first, marked by the lower arrow, evolves toward increased values of LDs independently of COSEn values, whereas the second one, highlighted by the upper

arrow, points toward both higher values of LDs and COSEn, reaching the maximum for both the indices

The results hint that heart rate dynamics, alone, can inform on the mortality risk. In particular, our results supports the idea that condition characterized by AF, high burden of ectopy and reduced variability are associated to mortality.

Discussion and Conclusion

This work proved the benefit of dynamical measures in the problem of arrhythmias detection and classification. COSEn and LDs were already tested as efficient measures to specifically detect AF and abnormal local dynamics, respectively (Lake and Moorman, 2011) (Moss et al, 2014). Furthermore, this work included the short-term scaling exponent obtained from DFA computed over 10-minute segments as a useful parameter to distinguish three very important clinical arrhythmias, such as NSR, AF and SR with a certain burden of ectopy. However, future improvements can be done by investigating different types of classification algorithms.

Our clinical emphasis constrains our analysis in several ways. First, we consider atrial flutter to be the same as AF. This approach, which is based on the similarities in clinical management, can certain lead to misclassifications with NSR. Second, we assigned the diagnosis of AF when as little as 30 seconds, or 5% of a 10-minute segment was present. This is consistent with clinical practice, where episodes lasting as in our case elicit full consideration in AHA guidelines (Fuster et al, 2006), and thus can lead to treatment measures as for AF. Finally, as previously stated, we assigned the diagnosis of ectopy when as little as 10% is present. The end result of these classification produced a diagnose of AF or SR with ectopy even when the rhythm is 90% or more purely normal SR.

An accurate arrhythmias detection and classification together with an effective method to determine the risk of the subject associated with the arrhythmias, both based only on RR interval time series, could have an important clinical impact for the management of hospitalized and ambulatory outpatients.

Moreover, the potentialities of an automatic RR-based arrhythmias classifier are enormously important in new growing fields as home care monitoring and telemedicine, where it could find extensive applications, but also in intensive care unit (ICU) setting. The potentiality of this analysis is represented indeed by its ability to work on segments of only 10 minutes, with an update of the values every 30 seconds, allowing it to be potentially useful in a clinical setting, where a continuous monitoring of the changes in cardiac rhythm and their relative risk is crucially important and can be life-saving. An example of the effectiveness of the classifier in a real time context is reported in Figure 2. The RR interval time series is depicted with dots, the line at the bottom represents the output of the classification model proposed in this thesis with an update performed every two minutes.

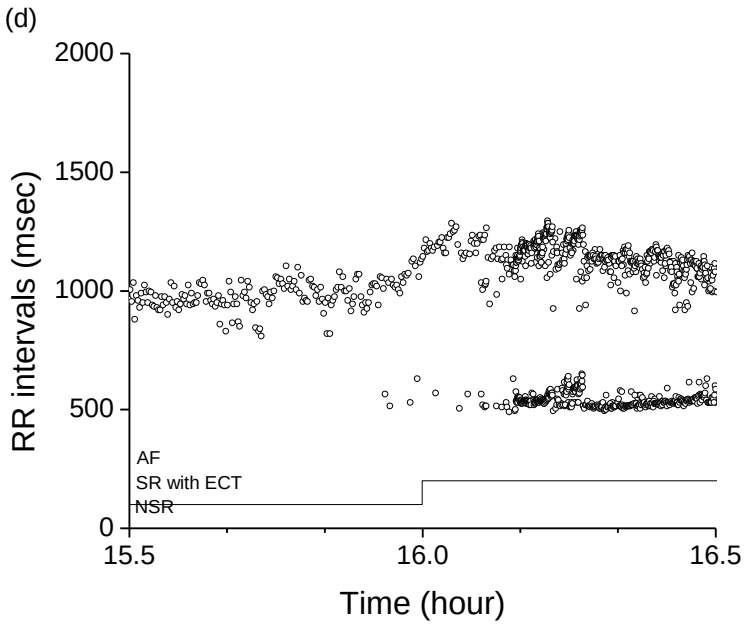

Figure 2. One hour segment of RR interval time series extracted from 24 hour Holter record. It is visible a transition from NSR to SR with ectopy, that the model (bottom solid line) efficiently tracks.

On the other hand, the idea of a "risk map" where regions of low, average and high mortality risk are depicted, can find interesting applications in clinical care too. The map permits to follow the patient course and to see if the therapy is able to maintain the patient or to bring the patient back to the safe region. The monitoring could be performed also real time.

Sommario

Introduzione

Le malattie cardiovascolari sono considerate una delle principali cause di mortalità nei paesi sviluppati, ed è stato stimato che più del 30% di tutti i decessi è associato ad esse (Go et al, 2013). Le contrazioni ventricolari premature (PVCs) sono responsabili di una prognosi negativa anche in assenza di difetti strutturali del cuore (Cha et al, 2012) (Lee et al, 2012), mentre le contrazioni atriali premature (PACs) precedono eventi di fibrillazione atriale (AF) (Haissaguerre et al, 1998) e sono considerati marker di episodi parossistici di AF in pazienti che hanno subito un ictus ischemico acuto (Wallmann et al, 2007). AF è stata riconosciuta come uno dei principali fattori di rischio di ictus ed è associata ad un generale aumento di morbidità e mortalità cardiovascolare (Benjamin et al, 1998) (Wolf et al, 1991) (Stewart et al, 2002). Data la sua maggiore incidenza in pazienti anziani (Lake and Moorman, 2011) e il rapido invecchiamento della popolazione globale, diventa sempre più crescente il bisogno di dispositivi elettronici meno invasivi ed accurati per il rilevamento di episodi di AF.

La presenza di AF implica decisioni cliniche importanti, come terapie con anticoagulanti o la rimozione chirurgica dell'appendice atriale, cardioversione, ablazione e farmaci antiaritmici. Al contrario, quando sono presenti battiti prematuri, sia di origine atriale che ventricolare, ma non è stata diagnosticata nessun'altra patologia cardiaca, non viene prescritto nessun trattamento al paziente, anche se la percentuale di extrasistolie è molto elevata.

I dispositivi che sono presenti attualmente per il rilevamento delle aritmie cardiache, come per esempio l'ECG Holter, sono scomodi per il paziente e si basano sull'analisi del segnale ECG. Tuttavia il segnale ECG può essere molto rumoroso e affetto da artefatti, rendendo l'estrazione di parametri in questi casi complicata e spesso non praticabile.

La serie degli intervalli RR, al contrario, è un segnale affidabile, richiede un minor costo computazionale ed è meno soggetta al rumore.

Tuttavia, l'uso di strumenti non invasivi per il rilevamento del ritmo cardiaco non è molto diffuso a causa della bassa affidabilità dimostrata finora da questi dispositivi nel rilevare episodi di AF basandosi solo sul segnale RR. In letteratura sono presenti molti studi che documentano l'accuratezza dei metodi proposti per distinguere AF dal ritmo sinusale normale (NSR) basandosi sul fatto che le dinamiche dei due ritmi sono largamente differenti (Sarkar et al, 2008) (DeMazumder et al, 2013) (Lake and Moorman, 2011) (Tateno and Glass, 2001). Tuttavia, in presenza di un ritmo sinusale (SR) e un'alta percentuale di battiti prematuri, sia atriali che ventricolari, le caratteristiche del segnale possono confondersi con quelle di un segnale di AF.

L'obiettivo principale di questa tesi è di fornire un algoritmo per il rilevamento e la classificazione di AF anche in situazioni in cui siano presenti alte percentuali di battiti ectopici, basandosi solo sulle caratteristiche estratte da serie temporali RR. L'ipotesi di partenza è che indici legati alle dinamiche non lineari delle serie RR possano contribuire a una distinzione migliore tra AF e SR con battiti prematuri. Tre indici non lineari sono stati presi in considerazione. Il *Coefficient of Sample Entropy* (COSEn) è stato proposto per distinguere NSR da AF, condizione che presenta alti valori di entropia, ed il suo calcolo è stato ottimizzato per segnali molto brevi (Lake and Moorman, 2011). Il *Local Dynamics score* (LDs) è stato recentemente proposto come nuovo indice in grado di catturare le dinamiche locali non lineari del segnale RR, proprietà che sono legate alla variabilità cardiaca e alla presenza di battiti ectopici. Per ottenere un singolo valore di LDs sono necessari solamente 12 battiti (Moss et al, 2014). Infine la *Detrended Fluctuation Analysis* (DFA) è invece un metodo utilizzato per quantificare le proprietà frattali delle serie RR (Peng et al, 1995).

Il secondo obiettivo è di fornire un'analisi del rischio di mortalità nei 2 anni successivi all'esame sulla stessa popolazione, utilizzando solo le misure di COSEn e LDs. È stato ipotizzato che una combinazione delle informazioni derivanti dai due parametri non lineari potesse essere utile nel comprendere l'associazione tra la presenza di aritmie cardiache e il rischio di mortalità.

Materiali e Metodi

2’722 registrazioni Holter di 24 ore sono state raccolte alla *University of Virginia (UVa) Heart station* dal 12/2004 al 10/2010. Le serie RR sono state suddivise in 377’285 segmenti da 10 minuti e ciascun segmento è stato classificato come: AF se la percentuale di battiti classificati come AF era superiore al 5%; SR con battiti prematuri se la frequenza di extrasistolie era superiore al 10%; NSR in tutti gli altri casi. Il database risulta così composto: 79% di segmenti classificati come NSR, 8% come AF e 13% come SR con battiti ectopici. Le tre categorie sono mutualmente esclusive e rispecchiano la pratica clinica.

Per testare l’ipotesi che l’aggiunta di misure dinamiche non lineari contribuisse ad aumentare la performance della classificazione, sono state utilizzati diversi metodi. Il criterio generale è stato quello di confrontare l’accuratezza della classificazione basata solo sulla media e la deviazione standard delle serie RR rispetto alla stessa classificazione ottenuta con l’aggiunta delle tre misure non lineari – COSEn, LDs e il coefficiente DFA. Il primo metodo si basa su tre modelli di regressione logistica multivariata, ciascuno dei quali distingue un gruppo dagli altri due. Il secondo approccio usa l’approccio *k*-nearest neighbor (*k*-NN). Tutti i modelli sono stati validati utilizzando la procedura *10-fold cross-validation* sull’intero database. Infine, i modelli sono anche stati validati esternamente sul database MIT-BIH.

Gli indici media, deviazione standard, COSEn e LDs sono stati calcolati ogni 30 secondi e poi i valori sono stati mediati sui 10 minuti, mentre la DFA è stata valutata considerando l’intero spezzone da 10 minuti.

Per quanto riguarda l’analisi del rischio di mortalità, è stata stimata la densità della distribuzione congiunta delle variabili COSEn e LDs usando dei kernel multivariati. Il kernel selezionato ha caratteristiche gaussiane bivariate con una matrice di larghezza di banda diagonale, che permette un’attenuazione delle alte frequenze in ciascuna coordinata (Botev et al, 2010). La scelta dei due parametri di è stata ottimizzata e non prevede un modello parametrico per i dati (Lake, 2009).

Risultati

Il risultato principale consiste nel miglioramento della distinzione di SR con battiti prematuri grazie all'aggiunta delle misure non lineari. Il valore predittivo positivo sia nel caso del modello logistico che nel caso del modello *k*-NN è pari a 85% e i valori per la diagnosi di NSR e AF risultano anche più elevati, e pari rispettivamente a 96% e 90%. L'accuratezza cresce ulteriormente se la soglia imposta sulla percentuale di battiti ectopici, necessaria per classificare il segmento come SR con battiti prematuri, viene scelta superiore al 10%.

I risultati mostrano che le misure utilizzate in questo studio non sono in grado di distinguere tra SR con PVCs e SR con PACs, contrariamente a quanto ci si aspetterebbe. Una identificazione tra questi due ritmi è tuttavia clinicamente molto importante, in quanto i PACs possono essere precursori di un imminente episodio di AF, mentre i PVCs sono associati con un alto rischio di mortalità, soprattutto se in pazienti con malattie cardiache preesistenti. Per verificare questa ipotesi, 4 modelli di regressione logistica sono stati sviluppati per differenziare segmenti classificati come AF, NSR, SR con PVCs e SR con PACs, ma i risultati mostrano un'alta percentuale di errore nella distinzione delle due classi con battiti ectopici, cioè tra SR con PVCs e SR con PACs.

I modelli sono stati ulteriormente validati utilizzando i database MIT-BIH di NSR, AF e altre aritmie (ARH). In questa analisi i valori di predizione positiva nel caso di NSR e AF raggiungono percentuali pari rispettivamente a 99% e 96%, ma nel caso di SR con battiti prematuri i valori ottenuti sono peggiori. Ipotizziamo che questo sia dovuto alla bassa incidenza di segmenti classificati come SR con battiti prematuri nel database MIT-BIH, dove sono meno dell'1% di 11'196 segmenti da 10 minuti, mentre nel database UVA erano il 13% di 377'825 spezzoni

Infinte per quanto riguarda l'obiettivo secondario di indagare il rischio di mortalità entro 2 anni dall'esame Holter nella popolazione Holter UVa, solo pazienti con età superiore a 40 anni sono stati presi in considerazione e il risultato principale di questa analisi è una mappa del rischio mostrata in Figura 1.

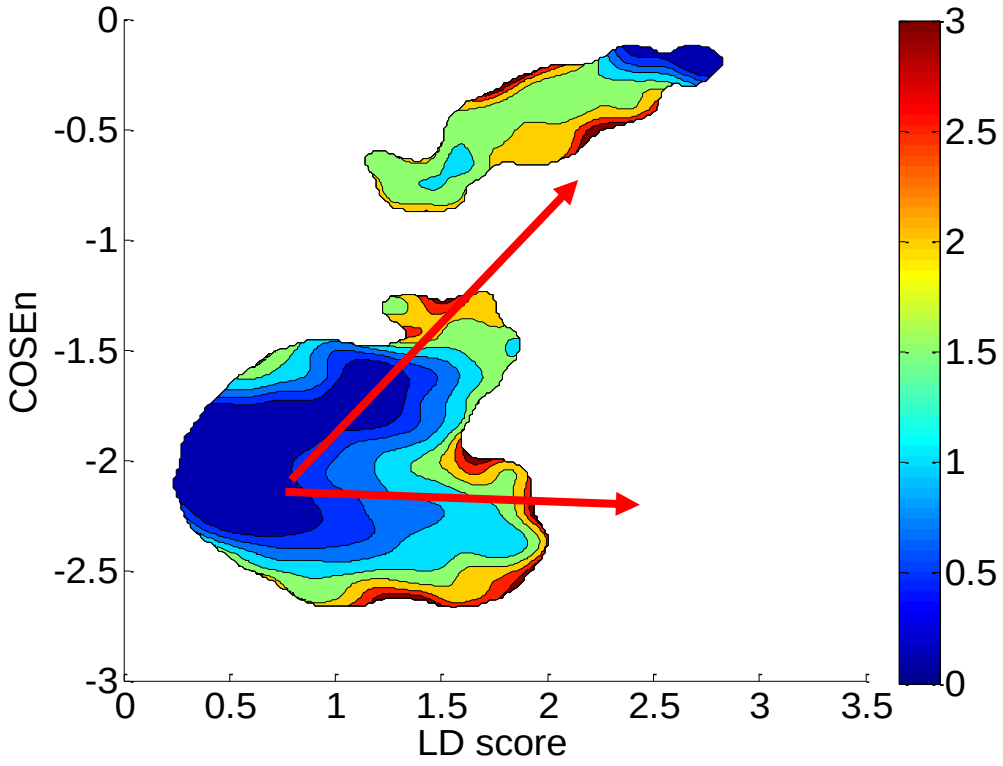

Figura 1. Rischio di mortalità entro 2 anni dall'esame Holter ECG nella popolazione Holter UVa

Si nota come la regione associata a un basso rischio di mortalità (blu scuro) è caratterizzata da bassi valori di LDs, mentre regioni a rischio di mortalità più alto sono contraddistinte da valori maggiori dell'indice. In particolare, partendo dall'area a basso rischio nell'angolo in basso a sinistra, è possibile notare due direzioni di aumento del rischio: la prima, indicata dalla freccia in basso, evolve verso valori crescenti di LDs indipendentemente dai valori assunti da COSEn; la seconda, indicata dalla freccia in alto, ha una direzione verso valori più alti di entrambi gli indici, raggiungendo la zona con i valori massimi.

Questi risultati suggeriscono che misure legate alle dinamiche non lineari del segnale di frequenza cardiaca contengono informazioni associate al rischio di mortalità e, in particolare, situazioni di AF, SR con ridotta variabilità e alta percentuale di battiti prematuri sono altamente associate ad un aumento di mortalità.

Discussioni e Conclusioni

In questo lavoro di tesi si è dimostrata la potenzialità di usare misure non lineari per ottimizzare la classificazione del ritmo cardiaco e identificare aritmie cardiache. Mentre parametri come il COSEn e LDs erano già stati validati come misure utili per l'identificazione rispettivamente di AF e dinamiche locali alterate (Lake and Moorman, 2011) (Moss et al, 2014), in questa tesi è stato proposto il coefficiente di breve scala ricavato dalla *Detrended Fluctuation Analysis*. Studi futuri possono avere come obiettivo quello di investigare diversi tipi di algoritmi per la classificazione a partire da questi stessi indici o addirittura includendo altri indici.

La forte impronta clinica di questo studio ha limitato l'analisi in diversi aspetti. Per prima cosa, i flutter atriale sono stati inclusi nella stessa classe dell'AF, in base al fatto che in entrambi i casi i medici prescrivono gli stessi trattamenti clinici. Tuttavia il flutter atriale è un ritmo che viene comunemente confuso con il ritmo NSR. In secondo luogo, è stata assegnata l'indicazione di AF a spezzoni con solo il 5% di battiti classificati AF, cioè 30 secondi in un segnale di lunghezza pari a 10 minuti, secondo le linee guida dell'American Heart Association secondo cui per un episodio parossistico di AF di durata 30 secondi viene consigliato un trattamento come per l'AF (Fuster et al, 2006). Infine, come precedentemente descritto, è stato assegnata la classificazione di SR con battiti prematuri anche quando solo il 10% dei battiti era identificato come prematuro. Entrambe queste scelte hanno portato alla diagnosi di AF o SR con battiti prematuri in casi in cui il ritmo è classificato per più del 90% come sinusale.

La possibilità di ricavare dall'analisi della sola serie RR una classificazione accurata delle aritmie cardiache e un metodo efficace per determinare il rischio del paziente in presenza di determinate aritmie, può avere un grosso impatto clinico per il trattamento di pazienti ospedalizzati e ambulatoriali.

Inoltre, le potenzialità di un classificatore automatico basato sul segnale RR sono rappresentate dall'applicazione in ambiti come l'*home care monitoring* e la telemedicina in crescente sviluppo, ma anche in ambiti come la terapia intensiva. La potenzialità di questa analisi risiede nell'abilità del classificatore proposto di funzionare con segmenti di 10 minuti e fornendo un aggiornamento dei valori dei

parametri ogni 30 secondi. Questo lo rende uno strumento utile in scenari clinici, dove un monitoraggio continuo dei repentini cambiamenti nel ritmo cardiaco e del rischio del paziente è d'importanza cruciale. Un esempio è mostrato in Figura 2, dove viene mostrata la serie RR (punti) e la linea nella parte bassa del grafico mostra l'uscita del modello di classificazione proposto in questa tesi, aggiornata ogni 2 minuti.

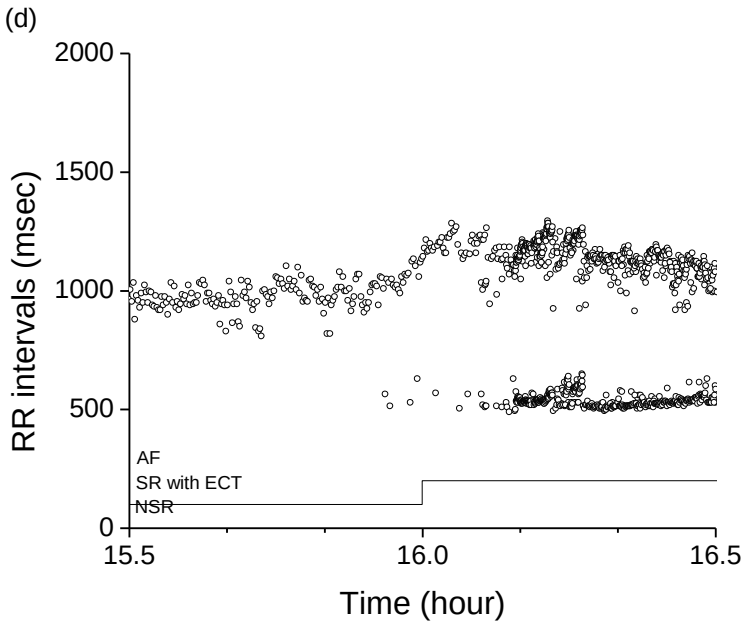

Figura 2. Spezzone di un'ora della serie RR estratta da una registrazione Holter di 24 ore. E' visibile una transizione da ritmo NSR a SR con battiti prematuri di cui il modello (linea inferiore nel grafico) riesce efficacemente a identificare.

Inoltre, anche la proposta di una "mappa di rischio" dove vengono rappresentate regioni di basso, medio e alto rischio può trovare applicazioni interessanti in ambito clinico. Questa mappa permette di visualizzare i miglioramenti o peggioramenti del paziente e verificare se certi trattamenti sono efficaci nel ridurre il rischio. Il monitoraggio può essere effettuato in tempo reale similmente al classificatore proposto.

.

Chapter 1

Introduction

1.1. Background and motivation

Several common clinical scenarios call for identification of cardiac rhythm in ambulatory outpatients. Atrial fibrillation (AF) is one of the most common chronic arrhythmia associated with an adverse prognosis, being an independent risk factor for increased cardiovascular morbidity and mortality (Benjamin et al, 1998) (Wolf et al, 1991) (Stewart et al, 2002). Its incidence is estimated to double with each successive age decade beyond 50 years, and it is greater in men than in women (Kannel et al, 1998). As reported by the World Health Organization (WHO) in 2012, the world's population is rapidly ageing, estimating a doubling of people over 60 years from about 11% to 22% between 2000 and 2050. In terms of absolute numbers, the expected increase is from 605 million to 2 billion. This situation claims for effective detection and monitoring of AF in a rapidly increasing part of the population, and the need of low-cost, accurate and comfortable devices for cardiac rhythm monitoring is emerging. AF is often paroxysmal in nature and decisions about its therapy are better supported by knowledge of the frequency, duration and severity of the arrhythmia (Prystowsk, 2000). While implanted devices can record this information with great accuracy (Ricci et al, 2009) (Hindricks et al, 2010), non-invasive diagnostic devices for ECG recording are limited by the need for skin electrodes and, while much smaller than in past years, these recording apparatus are obtrusive for the patients (Barret et al, 2014). Holter recording is a very common technique to monitor patients with cardiac disorders; it consists of a registration of a patient's ECG by means of a portable device, typically at least 24 h long or more. Because of the paroxysmal occurrence of AF, short ambulatory recordings are not sufficient to identify brief periods of arrhythmia, thus claiming for longer monitoring. Nonetheless, even high fidelity monitoring system as Holter device, can be limited by noisy and distorted

waveform data, which makes the features extraction from ECG waveforms not always feasible.

The most frequently available and reliable data is the series of the time intervals between two consecutive heartbeats or pulses, which is called RR interval time series. The analysis of this signal requires less computational cost with respect to the ECG feature extraction procedure and it's less affected by high frequency noise.

Since the 1980s, with the advent of chaos and information theory, the nonlinear and fractal behavior of heart rate (HR) signal has been investigated, beginning with the demonstration of self-similarity by Goldberger (Golberger et al, 1985). In the following years, many researchers began to analyze RR interval time series for clinical purposes (Braun et al, 1998) (Cerutti et al, 2007) (Ferrario et al, 2006). The idea, now widely accepted, is that the complex physiological variability of sinus rhythm (SR) is affected by age and illness and, thus, numerical analysis of RR series can help in clinical prognosis (Buchman et al, 2002) (Goldberger, 1996) by adding valuable information to traditional parameter. Many algorithms for analyzing RR interval time series exist (Acharya et al, 2006) (Bravi et al, 2011). These are usually classified in time domain, frequency domain, phase domain, non-linear dynamical domain, though Bravi et al (2011) have suggested a new classification into statistical, geometric, energetic, informational and invariant domains.

However, non-invasive devices for determining heart rhythm are not commonly used because of reduced confidence in detecting AF based only on the heart rate or RR interval time series. In fact, many methods to distinguish between AF and Normal Sinus Rhythm (NSR) has been proposed, given the largely different dynamics between the two rhythms (Tateno and Glass, 2001) (Sarkar et al, 2008) (DeMazumder et al, 2013) (Lake and Moorman, 2011), but situations of SR with frequent ectopy is expected to share features with AF, and thus to be distinguished with difficulty.

However these two conditions are treated very differently in clinical practice. Premature ventricular contractions (PVCs), alone, lead to poorer prognosis even in patients with no obvious heart disease (Cha et al, 2012). Indeed the cardiac

functionality improves after cardiac ablation in the great majority of patients with very frequent PVCs and low ejection fraction at the time of ablation (Yokokawa et al, 2013). However, no treatments are required even in situations with high burden of ectopic beats without concomitant pathological conditions such as cardiomyopathy. Premature atrial contractions (PACs), alone, don't have an important clinical impact but they may indicate a high risk of more severe atrial fibrillation or flutter. The remarkable difference between AF and SR with atrial or ventricular ectopy in terms of clinical implication claims for an accurate distinction of them, in order to give the adequate treatment to the patient and reduce the mortality.

1.2. Cardiac arrhythmias: pathophysiology and therapies

1.2.1. The electrical activity of the heart

The beginning of the sequence of stimulations, which is conducted over all the heart and allows it to contract, is placed in the sinus atrial node (SA node). It is a group of pacemaker cells approximately 2 mm thick and 8 mm long located between the right atrium and superior vena cava. These cells possess automaticity, which is the ability to depolarize without any external electrical stimulus. They spread a wave of depolarization through all the atria causing their contraction, called systole. The heart rate is the count of these contractions in a minute and it is determined by the duration of the depolarization and repolarization cycle of the SA node. The SA node maintains the heart rate regular, but there are a lot of outside sources that influence the electrical activity of the SA node. This extrinsic regulation of heart rate reflects the heart's ability to adapt to changing circumstances by detecting and quickly responding to unpredictable stimuli. The autonomic nervous system (ANS) plays the main role in this regulation governing the SA node through the parasympathetic (Vagus nerve) and sympathetic efferent. The ANS has indeed two contrasting components: the sympathetic and the parasympathetic nervous systems. The result of a sympathetic stimulation is an increase of the firing rate of the SA node and contractility of the heart, while the parasympathetic stimulation has an opposite effect. The first usually occurs in response to stress, exercise and heart disease, the second instead responds to the function of internal organs, trauma and allergic

reactions. The frequency band ranges of these two systems are different: low frequencies (0.04-0.15 Hz) are associated to sympathetic activation, while higher frequencies (0.15-0.4 Hz) are associated to parasympathetic firing.

After the atria, the pacemaker stimulus reaches the atrioventricular (AV) node. The AV node is a group of cells about 22 millimeters long, 10 millimeters wide and 3 millimeters thick that is located at the mouth of the coronary sinus between the right atrium and ventricle. For the electrical stimulus there isn't another way to be propagated to the ventricle. The purpose of this node is to reduce the speed of the impulse allowing the spilling of blood into the ventricles before their contraction, a heart cycle phase named diastole. The node is divided in three sections. Two of them allow the delay of the electrical pulse by means of the slow rate of conduction of the cells for one section and by means of a long pathway for the second one. The third section is the connection between the AV node and the Bundle of His. The AV node is also influenced by the ANS: the parasympathetic system can act prolonging the conduction through the AV node and, consequently, increasing the length of diastole and decreasing the heart rate; under intense parasympathetic stimulation, it can even happen to have a complete AV block. The sympathetic system, in contrast, decreases the conduction time through the node.

After the passage through the AV node, the electrical impulse is transmitted through the Bundle of His, which extends into the ventricular septum, and then it separates into the left and right bundle branches. These last branches formed the Purkinje system that conducts the electrical stimulus from the apex of heart upward through the ventricles (Figure 1.1). Once the impulse reaches these fibers, the systolic contraction becomes fully initiated.

This cycling propagation of the electrical impulse from the SA node, through the AV node, till the Purkinje fibers generating the contraction of the ventricles, can be recorded by the ECG, which has a characteristic waveform shown in Figure1.1. It is the result of the depolarization and repolarization of the four chambers of the heart in one cardiac cycle. The P wave refers to the depolarization of the atria, the QRS complex represents the depolarization of ventricles. The next T wave indicates the repolarization of the ventricles, while the atria's repolarization is hidden by the

higher amplitude of the QRS complex. The U wave is very small, so it is not always appreciable in ECG and it denotes the repolarization of the papillar muscles.

The physiological beating of the heart and, thus, the recurrence of this typical waveform is indicated as the so-called normal sinus rhythm.

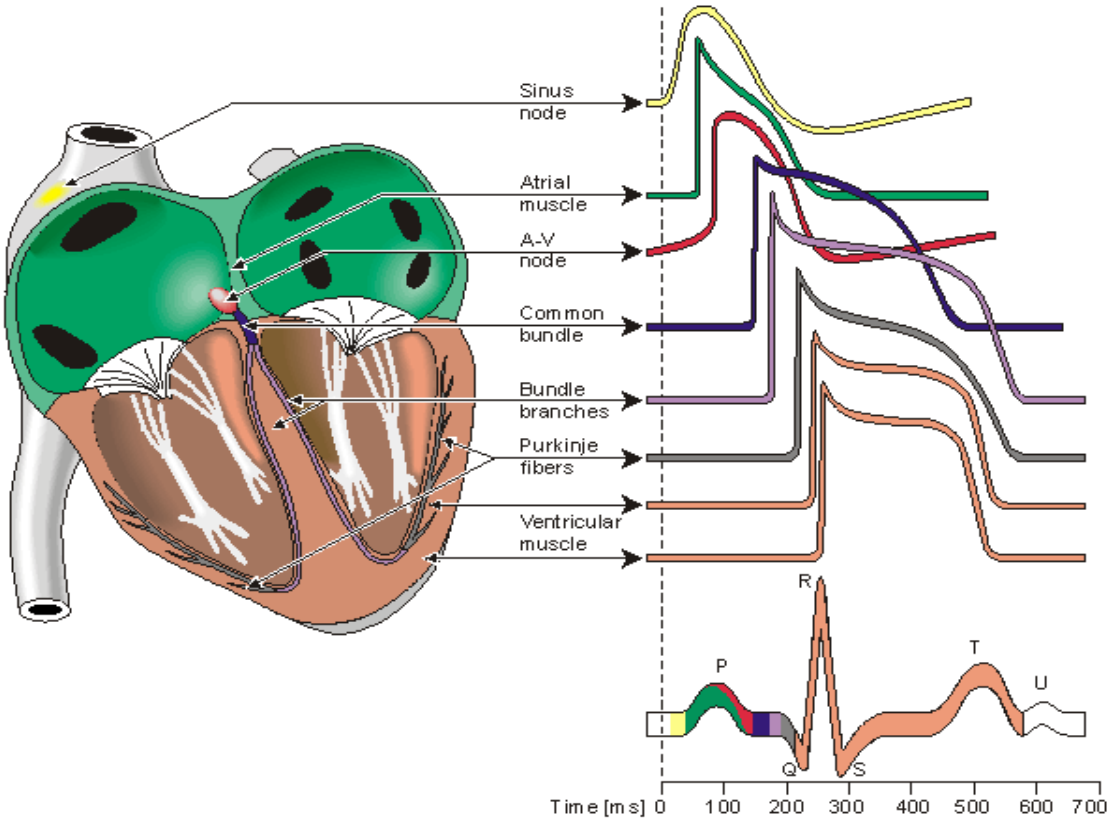

Figure 1.1 The electrical activity of the heart and the typical ECG waveform of a normal sinus rhythm

1.2.2. Pathogenesis of arrhythmias

Arrhythmia is a general term for any cardiac rhythm that deviates from normal sinus rhythm, caused by an irregular electrical activity of the heart. If the rhythm is faster it is called tachycardia, while if the heartbeat is slower than normal it is called bradycardia. Moreover, arrhythmias can be called atrial or ventricular based on where the arrhythmia has originated.

There are three basic mechanisms of pathogenesis of arrhythmias, regardless the specific type of arrhythmia: enhanced or suppressed automaticity, triggered activity, or re-entry. Automaticity is a natural property of all the cardiac cells to self-regulate and to initiate an impulse without an external stimulus. However, factors as aging, medications and others can alter this automaticity in different portion of the heart. For example, suppression of automaticity of the SA node can result in sinus node dysfunction, which is still the most common indication for permanent pacemaker implantation.

Triggered activity occurs when a series of heartbeats which spontaneously originate from afterdepolarizations, which are oscillations in membrane potential that follow the upstroke of an action potential. These can be of two types: early afterdepolarizations, occurring during the repolarization of the action potential, and delayed afterdepolarizations, which occur when the repolarization is complete or nearly complete. When the afterdepolarizations are large enough to reach the threshold, an action potential results, called triggered.

The most common mechanism of arrhythmogenesis is the re-entry. It is related to the process of re-excitement of the heart cells after the end of the refractory period due to impulses that fail to die out after normal activation of the heart. Re-entrant arrhythmias are defined as continuous repetitive circular propagation of excitatory waves, which return to their originating site and re-activate it. Atrial or ventricular fibrillation and tachycardia are generated by this mechanism.

1.2.3. Atrial Fibrillation

Atrial Fibrillation (AF) is considered the most common supraventricular tachycardia. About 2.2 million US citizens live with this condition and its incidence is estimated to double with each successive age decade beyond 50 years. After

adjusting for cardiovascular risk factors and predisposing conditions, the risk of AF was still found to increase 2-fold for each decade of aging and it was predominantly present in male than in female (Kannel et al, 1998).

During AF, the normal regular electrical pulses generated by the SA node are overcome by disorganized electrical pulses mostly originating in the left atrium and in the roots of the pulmonary veins. The atrial impulse rate can achieve about 300-600 beats per minute nullify the delay action of AV node because of the fast, chaotic and irregular nature of the impulses. This leads to an inadequate emptying of both atria and ventricles, due to the irregular and fast contraction rate. The inadequate emptying of the ventricles leads to a reduction of stroke volume causing symptoms as fatigue, breathlessness and chest pain, depending on the frequency and severity of AF.

The inadequate emptying of the atria allows blood to stagnate into the atria too. Within the left atrium there is an area called *atrial appendage* or *auricola*, due to an enlarged atrial muscle mass that forms a pouch, which usually works as decompression chamber during ventricular systole or when the atrial pressure is too high. During AF, the atria are not able to empty and this leads to clot formation in the appendage. When a blood clot breaks away, the risk of embolism and of an embolic stroke is very high (Wolf et al, 1991). Moreover, because the blood stagnates, the atria become enlarged with time and this may be a predisposing factor for permanent AF condition in adult patients or dilated cardiomyopathy.

An AF episode can last from minutes to days or can even be permanent. In the first case, if the episode self-terminates in less than 7 days, it is called *paroxysmal AF*. On the contrary, if the event lasts for more than 7 days it is classified as *persistent AF*. If there is an ongoing long-term episode (i.e. a year or more) the AF is categorized as *permanent*. Episode that last less than 30 seconds are not included in this classification. This classification was recommended by the American College of Cardiologist (ACC), the American Heart Association (AHA) and the European Society of Cardiology (ESC).

AF is generally associated with underlying cardiac diseases. Usually a damage of the heart tissue may generate extra impulses, whereas stretching and

remodeling of the cardiac muscle tissue may increase atrial pressure, and consequently the pressure on the pulmonary veins. This may be a contributing factor to other contributing causes to AF such as atherosclerosis, heart failure, hypertension, coronary heart disease, valve disease and congenital heart disease (Cottrell, 2012).

For patients with AF, clinicians need to accurately evaluate prescription of oral anticoagulation and to decide the monitoring process of the patient, i.e. rate and type of examinations. Rhythm control is necessary to verify symptoms, prevent tachycardia-induced cardiomyopathy due to the high ventricular rate and prescribe therapy to restore normal sinus rhythm.

Cardioversion is the typical medical procedure to restore the abnormal rhythm to the normal sinus rhythm. The synchronized electrical cardioversion consists in the electrical shock sent to a portion of the heart at a specific phase of the cardiac cycle, commonly in correspondence of R peak. The pharmacological cardioversion consists in giving specific antiarrhythmic agents to the patient. Drugs like amiodarone, diltiazem, verapamil and metoprolol are frequently given before cardioversion to decrease the heart rate, stabilize the patient and increase the chance that cardioversion is successful

The increased risk of stroke associated with the presence of AF requires specific antithrombotic treatments, as oral anticoagulants, among which the most common is warfarin. The implications for anticoagulation therapy alone are enormously important, as the rate of stroke rises sharply with even short episodes of AF (Healy et al, 2012). These therapies have been shown to lower the risk of clinical thromboembolism in all patients with AF, regardless of the type (paroxysmal, persistent or permanent) (Hart et al, 2007). However, the bleeding risk associated to anticoagulant therapy can exceed the risk of thromboembolism without therapy in the lowest-risk patients, thus, the initiation of antithrombotic treatment requires an accurate evaluation of both embolic and bleeding risk (Levine et al, 2001).

AF is usually diagnosed by the absence of the P waves in an ECG trace. P waves represent the atria depolarizations and in this case they are replaced by an irregular ventricular rate, as shown in Figure 1.2.

Figure 1.2 ECG of a patient in AF

1.2.4. Atrial Flutter

Atrial flutter (AFL) is usually associated with a fast heart beat and it falls in the supraventricular tachycardia category. The origin of AFL is usually a premature electrical impulse arising in the atria, which propagates due to the differences in refractory periods of atrial tissue. The electrical signal travels in an organized circular motion within the atria, causing them to beat faster than the ventricles. But not all the impulses risen in the atria reach the ventricles, thanks to the low-pass filtering action of the AV node, which limits the maximum heart rate. Flutter rates can reach even 300-400 bpm, but only a portion of these impulses reach the ventricles based on the stable n : 1 conduction regime of the AV node. For this reason AFL gives rise to a very fast and regular heart rate, completely different from AF, although AFL requires the same treatment. Usually it develops in adults with various types of heart disease or severe pulmonary disease and after cardiac surgery (Kastor, 2002). Figure 1.3 shows the ECG signal of a patient with AFL.

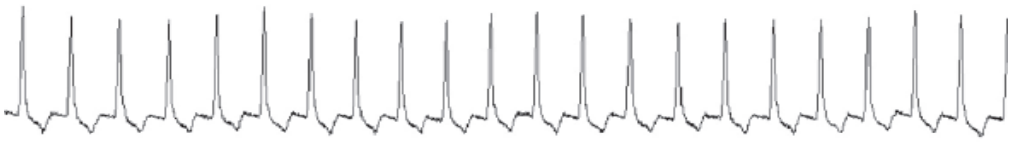

Figure 1.3 ECG of a patient in AFL

1.2.5. Premature Atrial Contractions

Premature Atrial Contractions (PACs) are produced by abnormalities of the atrial electrical activity, which lead to early contractions of the atria before the normal impulse from the SA node. The morphology of the P wave is abnormal, reflecting its origin in a different location than in the sinus node. Typically, the impulses propagate normally through the AV node generating narrow QRS complexes with a regular morphology. PACs, alone, don't have a big clinical importance and often they don't require specific treatments, but they may indicate a high risk of more severe atrial arrhythmias, such as AF or AFL. Figure 1.4 shows the ECG signal of a patient in SR with PACs.

Figure 1.4 ECG of a patient in sinus rhythm with PACs

1.2.6. Premature Ventricular Contractions

Premature ventricular contractions (PVCs) are contractions of the ventricles due to an impulse started in the Purkinje fibers rather than in the SA node. In this situation, ventricles contract before the atria when they are not still filled, leading to a reduced stroke volume. The ECG waveform is characterized by a normal beat followed by a fast extra beat (the PVC), a slight pause, and a following beat more forceful than normal. This is due to the fact that the ventricle fills with more blood during the pause after the premature contraction, giving the next beat extra force. When looking to the ECG trace a PVC event is easily seen by the spacing from the QRS complex preceding the PVC, which is shorter than normal (i.e. the premature contraction), and the QRS complex following the event which is much longer than usual (i.e. the compensatory pause) and of larger amplitude. However, the total duration of the short premature beat and its compensatory pause lasts as two consecutive normal beats.

They can be occasional or persistent, leading in the latter case to typical pattern as bigeminy, when premature beats alternate with sinus beats, trigeminy, when a premature beat follows two normal beats, or quadrigeminy, when one every four beats is premature. Couplets and triplets are sequences of a normal beat followed by two or three abnormal beats, respectively, and when three or more consecutive PVCs occur at a rate greater than 100 bpm the rhythm is classified as non sustained tachycardia.

PVCs are a common arrhythmia that everybody could occasionally have (in healthy hearts 4% of the population has more than 100 PVCs/day (Lee et al, 2012)), but usually they are more frequent in patients with hypertension, cardiomyopathy, pulmonary disease, congenital heart disease, cardiac surgery and an important myocardial damage (Kastor, 2002). Figure 1.5 shows the ECG signal of a patient in SR with PVCs.

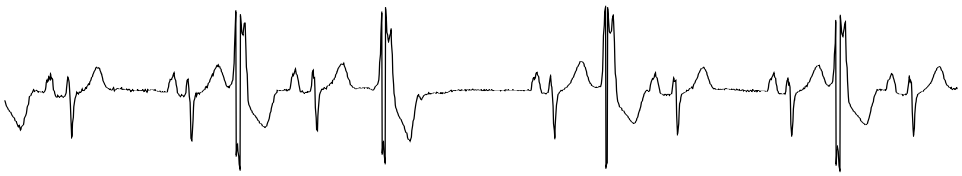

Figure 1.5 ECG of a patient in sinus rhythm with PVCs

1.3. Cardiac arrhythmias: mortality risk

Cardiovascular diseases are the leading cause of death in most of the developed countries, being associated with more than 30% of all deaths (Go et al, 2013). Therefore, there is a great interest in studying the underlying etiology of cardiac arrhythmias and new methods to improve their detection and classification, in order to prevent and treat the disease in advance, reducing the high burden of mortality.

AF is generally accepted as the most common chronic arrhythmia associated with an adverse prognosis, being an independent risk factor for increased cardiovascular morbidity and mortality. Clinical investigations revealed the significant association of AF to increased mortality risk, after adjusting for

coexistence cardiac conditions and common risk factors as age, hypertension, diabetes, left ventricular hypertrophy, myocardial infarction, congestive heart failure, valvular heart disease and stroke (Benjamin et al, 1998) (Krahn et al, 1995) (Stewart et al, 2002).

The relationship between AF and the risk of stroke, in particular, has been widely investigated. Together with hypertension, coronary heart disease and cardiac failure, which are well-known causes for stroke, AF was found to increase about five folds the risk of stroke, compared to the two, three and four folds related to coronary heart disease, hypertension and cardiac failure, respectively (Wolf et al, 1991). The high incidence of AF in old patients leads to a strong relation between AF and stroke especially in elderly, for whom all the other cardiovascular comorbidities become secondary factors.

Premature ventricular contractions have been thought for a long time to be relatively benign in absence of structural heart disease. Their effect on patients who have suffered myocardial infarction and in ambulatory patients with stable coronary heart disease has been widely studied. These works proved their strong relation with an increased mortality due to sudden and non-sudden cardiac death (Ruberman et al, 1981) (Moss et al, 1979) (Chugh et al, 2008). However, over the last decade, PVC-induced cardiomyopathy and left ventricular dysfunction has been subject of a great interest as many works proved this evidence (Cha et al, 2012) (Lee et al, 2012). Moreover, a recent research explored the relation between premature cardiac contractions and risk of incident ischemic stroke, resulting in an association of PVCs and PACs with a 2- and 1.3-fold increase in the rate of ischemic stroke, respectively (Ofoma et al, 2012).

The incidence of cardiac arrhythmias and their association with death have been investigated for many years even on critically ill hospitalized patients, especially those admitted in the Intensive Care Unit (ICU). Studies about the impact of arrhythmias in pediatric cardiac ICU (Hoffman et al, 2002), in the surgical ICU (Knotzer et al, 2000), in the medical ICU (Arrigo et al, 2013) (Khoo and Lip, 2009) (Reinelt et al, 2001) and on premature infants in the neonatal ICU (Southall et al, 1982), reveal the importance of arrhythmias in this clinical setting. The most common are supraventricular tachyarrhythmias as AF or AFL and ventricular

arrhythmias such as ventricular fibrillation or tachycardia. Furthermore many ICU patients experience more than one arrhythmias type (Hoffman et al, 2002). An overall increase in mortality risk in critically ill and arrhythmic patients was observed universally, explaining the urgent necessity of detailed etiological studies about cardiac rhythm abnormalities and methods to accurately detect them in many clinical setting and ambulatorial facility.

1.4. Cardiac Arrhythmias: detection algorithms

The strong relation between arrhythmias and mortality risk makes the clinical diagnosis of them extremely important, as discussed in the previous paragraphs, and this pushed researchers to develop new methods for the automatic detection and classification of various arrhythmias.

The majority of them are based on the analysis of the ECG morphology, being a non-invasive and low-cost method, which provides important information regarding the rate and the regularity of the heart. However, the extraction of ECG features for detection and classification of arrhythmias is not always feasible due to the presence of noise, which often makes the analysis on the ECG signal very difficult, and to the time-consuming computational process, which becomes thus ineffective for real time analysis.

Alternative approaches to the problem have been proposed, based on the direct analysis of the RR intervals time series. Although the high computational velocity and the absence of ECG noise allow these new techniques to be more efficient than the ECG-based algorithms, an important drawback is associated with the effectiveness of the QRS detector algorithm. However, sophisticated algorithms have been developed allowing a precise detection of the R peaks within good confidence intervals.

A good reason to prefer a RR-based arrhythmias classifier than an ECG-based algorithm is the fact that diagnostic ECG waveform may not always be available, especially in ambulatory monitoring, while the heartbeat can be easily detected in every clinical setting.

1.4.1 ECG based classification algorithms

Common features extracted from the ECG signal include frequency-based features (Minami et al, 1999), time frequency-based features (Tompkins, 1995), non-linear features such as Lyapunov exponent and the correlation dimension (Owis et al, 2002), ECG morphology features such as ST segment area, RS interval, ST slope, QRS area and R-wave amplitude (Chazal and Reilly, 2004) (Hosseini et al, 2006) (Cheng and Chan, 1998), Karhunen–Loeve expansion of ECG morphology (Moody and Mark, 1990) and wavelet transform (Senhadij et al, 1995) (Song et al, 2005) (Yu and Chen, 2008).

Recent methods for cardiac arrhythmias detection and classification employ neural networks (Minami et al, 1999) (Hosseini et al, 2006) (Yu and Chen, 2008) (Wang et al, 2001), hidden Markov models (Cheng and Chan, 1998), Linear or Quadratic Discriminant function (Chazal and Reilly, 2004) (Ouelli et al, 2012) and support vector machine (Song et al, 2005).

1.4.2 RR based classification algorithms

Using RR intervals time series for arrhythmias classification has lots of advantages, but few works have been done in this direction. A summary of them is presented in Table 1.1. The majority takes into account AF only, except two studies from Tsipouras et al (2004) and Kamath (2012). Moreover very few works admit atrial and ventricular ectopy. Only Huang et al (2011) and Bardossy et al (2013) consider both situations with PVCs and PACs. The first employed linear measures to identify the transitions between AF and NSR, whereas the second proposed a diagnostic algorithm for implantable cardioverter defibrillators. The second one reaches a very high accuracy, but the real innovation of that work consists in applying a new fuzzy logic-based scheme to standard measures of onset and instability. Tsipouras and Fotiadis (2003) proposed an automatic arrhythmia detector based on time and time-frequency domain analysis of the RR intervals. However, their method was designed to classify the input segment as “normal” or “arrhythmic” only without discrimination among the arrhythmias. Acharya et al (2002) employed an artificial neural network and a fuzzy equivalence classifier, combining linear and non-linear parameters, which could only classify the input segments into one of the

four different arrhythmia classes – ischemic cardiomyopathy, complete heart block, NSR and sick sinus syndrome together with AF and ectopy - without discrimination between AF and ectopic beats. The rest of the works listed in Table 1.1 consider only PVCs.

Linear and nonlinear measures are employed together with a variety of classification algorithms. The majority of these methods are tested on the canonical MIT-BIH database, which is relatively old and limited (free at http://www.physionet.org).

The classifier proposed in the present thesis was performed on a larger and more complex database of 2’722 24-hour Holter recordings collected at the University of Virginia (UVa) Heart Station from 12/2004 to 10/2010. The classifier was successively validated on the MIT-BIH database.

Table 1.1 List of works on RR-based classification algorithms

Reference	Database	Method	AF	Ectopy	NSR
(Tateno and Glass, 2001)	MIT-BIH	Linear measures, two-samples KS test	yes	-	yes
(Sarkar et al, 2008)	MIT-BIH	Linear measures	yes	-	yes
(Huang et al, 2011)	MIT-BIH	Linear measures	yes	Atrial and ventricular	yes
(Bardossy et al, 2013)	MIT-BIH and ICD database	Linear measures, Fuzzy logic	yes	Combined atrial and ventricular	yes
(Acharya et al, 2002)	?	Linear measures, ANN and Fuzzy classifier	yes	Yes	yes
(Tsipouras et al, 2004)	MIT-BIH	knowledge-based deterministic automaton	-	Ventricular	yes
(Tsipouras and Fotiadis, 2003)	MIT-BIH	Linear measures, ANN	yes	Yes	yes
(Lian et al, 2011)	MIT-BIH	Linear measures, RdR map	yes	Ventricular	yes
(Acharya et al, 2008)	Database from Kasturba Medical College Hospital, Manipal, India	Linear measures, ANN	yes	Ventricular	yes
(Acharya et al, 2004)	MIT-BIH	Linear and nonlinear measures	yes	Ventricular	yes
(Yaghouby et al, 2009)	MIT-BIH and MVAD databases	Linear and nonlinear measures, feature reduction with GDA and MLP-NN	yes	Ventricular trigeminy	-
(Anuradha and Reddy, 2005-2008)	MIT-BIH	Nonlinear measures, Fuzzy classifier	yes	Ventricular	yes
(Kamath, 2012)	MIT-BIH	Nonlinear measures, ANCOVA and NN	-	Ventricular	yes
(Acharya et al, 2003)	MIT-BIH	Nonlinear measures, Fuzzy classifier and ANN	yes	Ventricular	yes
(Mohammadzadeh Asl et al, 2008)	MIT-BIH	Linear and nonlinear measures, feature reduction with GDA and SVM	yes	Ventricular	yes
(Lake and Moorman, 2011)	UVa Holter	Nonlinear Entropy	yes	-	yes
(DeMazumder et al, 2013)	ICD database	Nonlinear Entropy	yes	-	-
This paper	UVa Holter	Linear and nonlinear entropy, kNN and logistic regression	yes	Atrial and ventricular	yes

KS=Kolmogorov-Smirnov, ANN=Artificial Neural Network , GDA=Generalized Discriminate Analysis, MLP-NN=Multi Layer Perceptron Neural Network, ANCOVA=Analysis of Covariance, SVM=Support Vector Machine, kNN=k-Nearest Neighbors

1.5 Objectives

The first and principal objective of this thesis was to provide an algorithm for the detection and classification of AF even when a very high burden of atrial and ventricular ectopic beats is present, based only on RR intervals time series. We hypothesized that indices related to dynamics of RR series can contribute to a better distinction of SR with ectopy from AF. We tested the hypothesis using three nonlinear indices. The Coefficient of Sample Entropy (COSEn) was designated to quantify the higher entropy characteristics of AF with respect to NSR, and the algorithm was optimized for very short time series (Lake and Moorman, 2011). Local Dynamics score (LDs) is a new index proposed to capture local dynamics of the heart rate, that are related to the baseline variability and to the outliers, such as ectopy (Moss et al, 2014). Detrended Fluctuation Analysis (DFA) is a well-known method to quantify the fractal-like scaling properties of the RR interval times series (Peng et al, 1995).

The second objective was to analyze the mortality risk of the same population, based on COSEn and LDs indices only. We hypothesized that the combination of these two entropy-based dynamical measures could help to shed light on association between cardiac arrhythmias and mortality risk.

The general goal of our work was to contribute to the clinical problem of AF detection and management of outpatients, and secondly to study mortality risk associated to arrhytmias in a large population composed of 2'722 24-hour Holter recordings from ambulatory patients with a follow-up of two years.

Chapter 2

Cardiac rhythm classification from RR intervals

2.1 Introduction

Since the 1980s, the rhythm of heartbeats has been contemplated as the output of a non-linear dynamical system. Mathematical tools of chaos theory and its precedents have been brought to bear on RR interval time series. Subsequently, a rich literature tests the idea that sophisticated numerical analysis of RR interval time series informs on clinical prognosis. The general finding, now clear and simple, is that the physiological variability of sinus rhythm has complex structure that gets lost with age and illness (Goldberger, 1996) (Buchman et al, 2002).

Another utility of dynamical systems analysis is in the detection of cardiac arrhythmia in clinical practice. The simplest and most intuitive application is the detection of AF, which has grossly different dynamics from sinus rhythm. This is important in clinical care, as this diagnosis leads to numerous decisions about stroke prevention with anticoagulation or left atrial appendage exclusion, rate control, cardioversion, ablation, and antiarrhythmic drugs.

Successful numerical methods for this purpose include inspection of Poincarè plots (Sarkar et al, 2008) and entropy estimation, as COSEn (Lake and Moorman, 2011). The latter work showed that RR interval time series in AF had higher entropy as expected. However, there are two challenging situations: atrial flutter, where entropy is low, but all the AF management problems still pertain, and SR with ectopy, both atrial and ventricular, where entropy is high, but not due to AF, and the therapy is different from AF.

The hypothesis of this work is that further analyses of the dynamics should allow better distinction of SR with ectopy from AF. The hypothesis was tested using two other dynamical techniques selected for their ability to detect the fundamental feature of SR with ectopy, that is, a baseline of normal variability punctuated by outliers. The first one is the Detrended Fluctuation Analysis (DFA), a well-characterized measure, examines variability from the mean at different time scales, and the second one is the Local dynamics score (LDs), a new index to measure variability and to detect outliers. We tested the proposed algorithms in a new database of 2'722 consecutive Holters from the University of Virginia, and validated them in the canonical MIT-BIH databases (Goldberger et al, 2000). The product – robust numerical recipes for distinguishing among NSR, SR with ectopy, and AF – are widely applicable in clinical practice, and should improve AF management.

2.2 Study population

We studied RR interval time series from 24 hour Holter recordings collected from 2'722 consecutive patients at the University of Virginia (UVa) Heart Station from 12/2004 to 10/2010. The age of the patients varied from 0 to 100 years, with an average value of 47±25 years. AF, PAC and PVC labels were obtained from an automatic classifier (Philips Holter Software). The RR series were subdivided into 377'285 10-minute segments. Each 10-minute segment was classified as AF if the burden of AF was greater than 5%, as SR with ectopy if the burden of PAC or PVC was more than 10%, as NSR otherwise. Thus, the dataset is composed of 79% NSR, 8% AF and 13% SR with ectopy segments. The 3 categories are mutually exclusive and reflect clinical practice.

2.3 Heart rate metrics

We computed means and standard deviations (SD) for 30-second segments and averaged results for each 10-minute segment. To investigate the HR dynamics, we computed the Coefficient of Sample Entropy, the slope from the Detrended Fluctuation Analysis and the Local Dynamics score.

2.3.1 Coefficient of Sample Entropy (COSEn)

COSEn is an entropy measure derived from the Sample Entropy (SampEn) and designed specifically to detect AF in very short RR interval time series (Lake and Moorman, 2011).

The idea of entropy was first proposed by Shannon (1948) as a part of communication theory and, in the following years, it was studied and re-elaborated in the works of Kolmogorov (1959/1959), Sinai (1959), Grassberger and Procaccia (1983), Eckmann and Ruelle (1985) and others. Pincus in 1991 proposed Approximate Entropy as a feasible method to be applied even to limited and noisy time series, as encountered in cardiovascular or other biological studies (Pincus, 1991). However, it has some limitations that were studied by Richman and Moorman (2000) who came up with a new entropy measure, called Sample Entropy (SampEn). This has the advantage of being less dependent on time series length and it shows relative consistency over a broader range of possible parameters, as tolerance, length of templates and the total length of signal.

Generally, entropy estimators measure the degree of regularity of a signal by counting how many template patterns repeat themselves. Repeated patterns imply order and lead to low values of entropy. More formally, sample entropy is the negative natural logarithm of the conditional probability that two sequences of length m that match within tolerance r will also match at the (m+1)th point. Given a data record of N consecutive interbeat intervals, $x_1, x_2, \ldots, x_n$, for a length $m < n$ and starting point i, the template $x_m(i)$ is the vector containing the m consecutive intervals $x_i, x_{i+1}, \ldots, x_{i+m-1}$. Defined a matching tolerance r, a template match occurs when all the components of $x_m(i)$ are within a distance r of any other $x_m(j)$ in the record. Let B_i denote the number of matches of length m within template $x_m(i)$ and A_i denote the number of matches of length $m + 1$ within template $x_{m+1}(i)$. We indicate with

$A = \sum A_i$ the total number of matches of length $m + 1$ and with $B = \sum B_i$ the total number of matches of length m. The ratio $cp = A/B$ is the conditional probability that subsequent points of a set of closely matching m intervals also remain close and match. The Sample Entropy is the negative natural logarithm of this ratio and it is computed as:

$$SampEn = -\ln(cp) = -\ln(A/B) = -\ln(A) + \ln(B) \quad (1)$$

If A and B are equal, which means that the time series is very regular, the entropy measure is zero, whereas if A is smaller than B, this leads to a higher value of entropy.

The choice of the parameters m and r is crucial in order to obtain a reliable estimation of the conditional probability, especially in very short time series. In fact, a too large value of m or a too small value for r brings to a very small number of matches, not sufficient for a confident result. On the other hand, both situations of a too large r or a too small m allow all the template to match each other, without discrimination among different rhythms. Lake proposed the conversion of the measured conditional probability to a probability density. The new measure was named Quadratic Sample Entropy (QSE) and it consists of normalizing the sample entropy by the volume of each matching region, $2r^m$ (Lake, 2006). In the calculation of entropy this reduces to adding $\ln(2r)$ to the estimation, and the equation (1) becomes:

$$QSE = -\ln\left(\frac{A}{(2r)^{m+1}}\right) - \left(-\ln\left(\frac{B}{(2r)^m}\right)\right) = -\ln(cp) + \ln(2r) = SampEn + \ln(2r) \quad (2)$$

QSE allows direct comparison of results obtained by using different values of r. Regression analyses showed that heart rate was an important independent predictor of AF (Lake and Moorman, 2011). Hence, the COSEn measure requires the subtraction of the natural logarithm of the mean RR interval:

$$COSEn = SampEn + \ln(2r) - \ln(mean\ RR\ interval) \quad (3)$$

In this work the choice of *r* and *m* reflects the standards and findings already described in (Lake and Moorman, 2011), therefore we chose *m* = 1 and *r* = 30 msec. We calculated COSEn over 30-second segments, consistent with the clinical idea that AF must usually last 30 sec to be considered (Fuster et al, 2006).

2.3.2 Detrended Fluctuation Analysis (DFA)

DFA was proposed by Peng et al. (1995) as a way to quantify the fractal-like scaling properties of RR interval time series and it is a measure of the complexity of a signal. The idea of complexity cannot be merely related to the concept of irregularity of a signal: the latter is linked to how patterns repeat themselves, but it lacks of information about the underlying process. Instead, complexity is associated with "meaningful structural richness" which, in contrast to the outputs of random phenomena, can also exhibit relatively high regularity. Entropy measures, as discussed above, assign the highest value to uncorrelated random signals such as white noise, which are highly unpredictable but not structurally complex and, at a general level, admit a very simple description. In a biological contest, the idea of complexity is related to the physiological complexity ,which is the capacity of the organism to adapt to the ever-changing environments, thus requiring an integrative and multiscale functionality. The so called "regular sinus rhythm" is, in reality, the result of the complex and erratic fluctuations of the interbeat intervals, exhibiting long-range correlations. Thus, a disease situation is seen as an alteration of this scale invariant (fractal) correlation property. The Detrended Fluctuation Analysis was proposed by Peng to quantify this quantity.

DFA computes the root-mean-square fluctuation of integrated and detrended time series F(*n*) for different window lengths *n*. A detailed description of the method is reported. The interbeat intervals time series of total length N is first integrated,

$$y(k) = \sum_{i=1}^{k}[B(i) - B_{ave}] \quad (4)$$

where B(*i*) is the *i*th interbeat interval and B_{ave} is the average interbeat interval. Next, the integrated time series is divided into non overlapping boxes of equal length, *n*. In each box a least-squares line is fitted to represent the trend in that box. Let $y_n(k)$ be the *y* coordinate of the straight line. The integrated time series, y(*k*), is detrended by subtracting the local trend $y_n(k)$ in each box. The root-mean-square fluctuation of this integrated and detrended time series is:

$$F(n) = \sqrt{\frac{1}{N}\sum_{k=1}^{N}[y(k) - y_n(k)]^2} \tag{5}$$

This computation is repeated over all the box sizes. The results from each box length are averaged – fewer points contribute to the plotted value for higher *n*. Typically, F(*n*) will increase with the box size *n.* A linear relationship on a log-log plot of *F*(*n*) versus the box size *n* indicates the presence of power law (fractal) scaling. Under such conditions, the fluctuations can be characterized by a scaling exponent. In fact, if the data are long-range correlated, F(*n*) increases as a power–law with respect to *n*, $F(n) \sim n^{\alpha}$. Thus, the fluctuation scaling exponent can be determined by a linear fit on the log-log plot. For uncorrelated data, such as white noise, the scaling exponent is $\alpha = 0.5$. A slope larger than 0.5 indicates persistent long-range correlations. In contrast, $0<\alpha<0.5$ indicates an anti-persistent type of correlation. The slope equal to 1 is the theoretical value which corresponds to 1/f noise, and $\alpha = 1.5$ to Brownian noise.

One of the main advantages of this technique is its effectiveness to work even on very non stationary signals. It must distinguish between those fluctuations driven by uncorrelated stimuli due to changes in the environmental conditions, and those intrinsic fluctuations, which arise from the complexity of the system. Only the last ones pertains to long-range correlations. Thus, the effectiveness of the DFA algorithm lays in the idea of "detrending" the physiological time series to eliminate all the fluctuations that arise from the external stimuli and affect the signal at a determined scale (i.e. at the frequencies related to the stimuli).

The original calculation of the DFA was proposed for long signals, such as 24hr Holter ECG recordings (Peng et al, 1995), but it was used also in shorter interval time series (Shieh et al, 2006) (Pena et al, 2009) (Yeh et al, 2009). In this work the scaling exponent α was calculated on the 10-minute segments over the box size range of 4 to 12.

2.3.3 Local Dynamics score (LDs)

The LDs is a new index to investigate the local dynamics of short RR series (Moss et al. 2014). The innovative idea is to examine how often individual templates in a short series match each other not only according to the rhythm, but also according to the local dynamics of the signal. In the original work the authors examined the challenging situation of the coexistence of reduced heart rate variability (HRV) and ventricular ectopy. The other common HRV metrics, such as standard deviation, range and the pNN*x* family, failed due to the contrasting influences of the two features on the metrics. In contrast, local dynamics (LD) showed different values for signals of low HRV punctuated with ectopy from both NSR and AF, proving the potentiality of this index in capturing abnormal local HR dynamics.

Given a 12-beat segment, the algorithm consists mainly into counting the number of times each sample matches with the other 11 with a tolerance *r* of 20 msec. A histogram of the count of templates as a function of the number of matches is constructed. If no points match, a bar of 12 counts appears in the bin 0, and all the other bins are empty, when all 12 points match each other, the histogram will have a bar of 12 counts in bin 11. The LDs is computed as a linear combination of the values in bin 0, bin 10 and bin 11; the coefficients were normalized so as to sum to 1. A uniform distribution of matches, i.e. the counts in all bins are equal to 1, leads to LD score of 1. Lower scores imply a bell-shape histogram distribution, and higher scores imply a distribution concentrated on either or both extremes of the histogram.

Here, we calculated the score on the average 12-beat histogram in each 10-minute segment.

2.4 Statistical analysis

One way Kruskal-Wallis ANOVA was used to compare the index values among the three groups (NSR, AF, SR with ectopy) and post-hoc multiple comparisons were performed by the Wilcoxon rank-sum test using the Bonferroni correction. For this univariate statistical analysis only a single 10-minute segment from each patient was randomly selected. To test the overall hypothesis that dynamical measures were useful for rhythm classification, we used several schemes. The strategy was to compare the accuracy of classification using means and SD alone, and after addition of the dynamical measures (COSEn, LDs and slope of DFA). The first scheme was a system of 3 multivariate logistic regression models, each used to distinguish one rhythm class from the other two. The final classification of the RR intervals time series was obtained by using the highest probability estimate among the three models. The second approach was a k-nearest neighbor technique (Xiao et al, 2010). All models were validated using a 10-fold cross-validation procedure on the entire dataset. Finally, the indices were computed as previously described on the MIT-BIH database and used to test the proposed model.

2.5 Results

2.5.1 Overview of the computational procedure

We propose an example of the analysis to better explain the computational procedure for each parameter and for better understanding the results.

Figure 2.1 shows ECGs of four patients from the UVa Holter database. Four different rhythms are illustrated: NSR (*a*), AF (*b*), SR with PVCs (*c*) and SR with PACs (*d*).

Figure 2.1 ECGs from four patients of the UVa Holter database in NSR (*a*), AF (*b*), SR with PVCs (*c*) and SR with PACs (*d*).

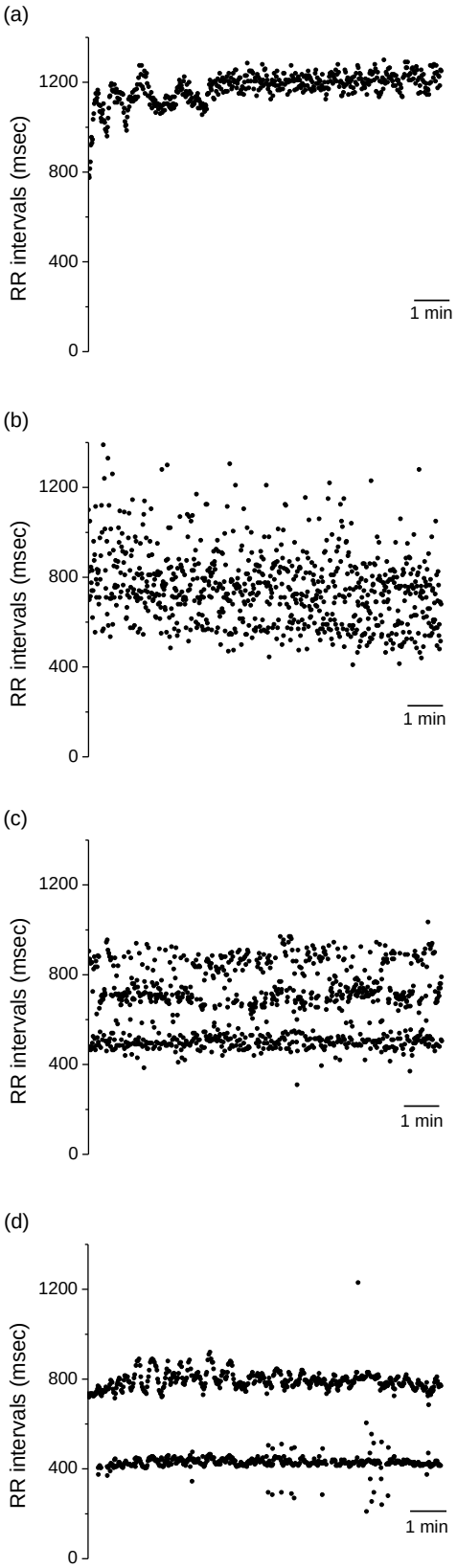

Figure 2.1 10 minutes of RR interval time series from the UVa Holter database for NSR (a), AF (b), and SR with PVCs (c) and PACs (d).

Figure 2.2 shows 10 minute segments of the RR interval time series from the same ECG recordings displayed in Figure 2.1. In this example we considered a 10-minute record of SR with a high burden of PVCs (Figure 2.2(*c*)) equal to 57% and a very high burden of PACs (Figure 2.2 (*d*)), equal to 73%.

Figure 2.3 illustrates an example of the procedure of counting matches, which is the core of the COSEn estimation, over the first 30 seconds extracted from the RR series of Figure 2.2(*a*). For a template of length $m = 1$ (first red filled circle) and a tolerance $r = 30$ msec (red lines), the number of matches is obtained by counting all subsequent points that fall within r, that is, within the tolerance range marked by the red lines. In this case only one match occurs and this is highlighted by the second red filled circle. Next, all the matches for a template of length $m+1$ (first red filled circle and first green triangle) are counted. The green lines delimits now the tolerance interval for the sample designed as a triangle.

A match occurs when all the points of the template are within a distance r of any other $m+1$ segment in the signal. Thus, in this case, there is only one match, which is highlighted by the shapes and colors. Finally, the natural logarithm of the ratio between the total number of matches of length $m+1$ and length m is divided by the factor $2r$, and subtracted by the natural logarithm of the mean of RR intervals. COSEn is so obtained.

The series depicted in Figure 2.2(*b*) is associated with the highest value of COSEn= -0.48, as the AF epoch is the most irregular signal, while an intermediate value characterizes SR with PVCs (COSEn = -1.29, Figure 2.2(*c*)), where the high burden of ventricular ectopy increases the low values of this index usually associated to NSR epoch. In fact, COSEn =-2.11 in NSR epoch (Figure 2.2 (*a*)) and COSEn =-1.82 was obtained for SR with PACs (Figure 2.2(*d*)). This results is expected for NSR, since the characteristic of this type of signal is its regularity, while in the case of SR with PACs it can be explained by the fact that high burdens of ectopic beats such as bigeminy, can lead to a very regular patterns.

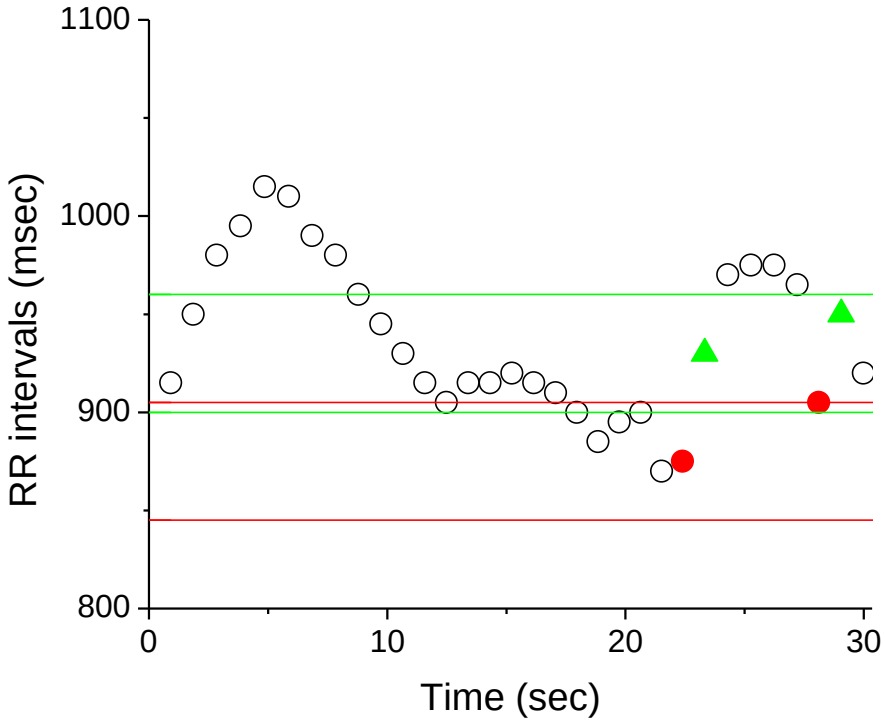

Figure 2.3 Illustration of the count of number of matches for template of length *m* and *m* +1, during COSEn calculation procedure. Here *m*=1 and tolerance *r*=30 msec. The red and green lines indicate the tolerance windows for the first red filled circle and the first green triangle, respectively.

Figure 2.4 shows an example of the detrending procedure for the DFA. Only the first 36 RR intervals of each trend in Figure 2.2 are shown and the detrending procedure is illustrated for box size *n*=4 and *n*=12. Note that the variations from the green lines are large, especially in panels (*a*) and (*b*).

Figure 2.5 shows the results for the 4 RR interval time series displayed in Figure 2.2. The 10-minute epochs classified as SR with PVCs and SR with PACs (line with triangles and line with circles) have a flat trend with a slope equal to 0.18 and 0.3, respectively. The epoch classified as NSR (line with stars) shows the trend with the highest slope, equal to 1.11. Finally, the trend classified as AF (line with squares) places in the intermediate region with a value of slope equal to 0.46 which is close to the theoretical value of 0.5 related to uncorrelated signals.

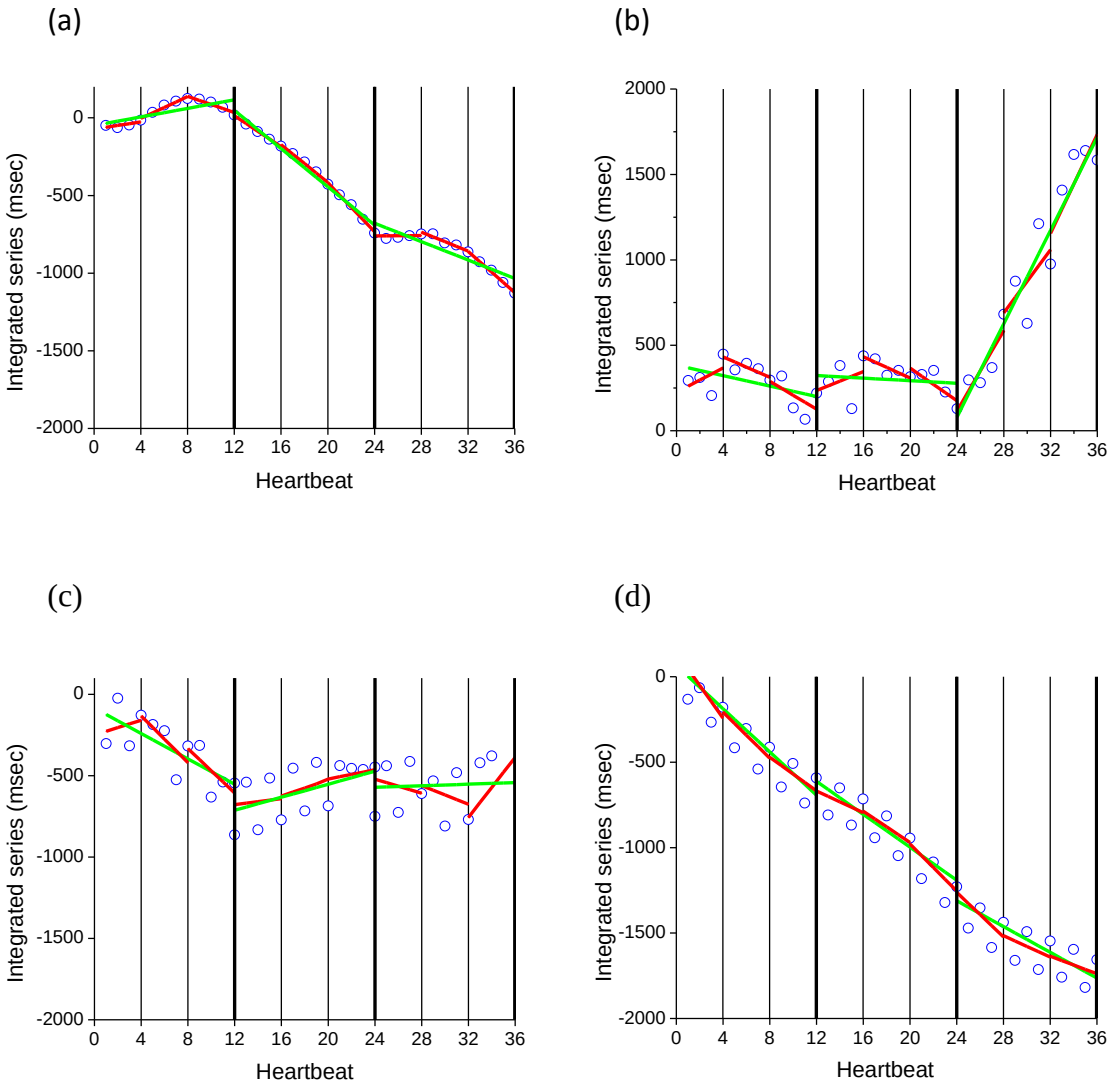

Figure 2.4 Illustration of the detrending procedure for the DFA in case of NSR (*a*), AF (*b*), SR with PVCs (*c*) and PACs (*d*) RR interval time series. The process is illustrated for the first 36 heartbeats of the 10-minute epochs shown in Figure 2.2. The open blue circles are the integrated signal, the red line and green line represent the linear interpolation for box size n=4 and n=12, respectively.

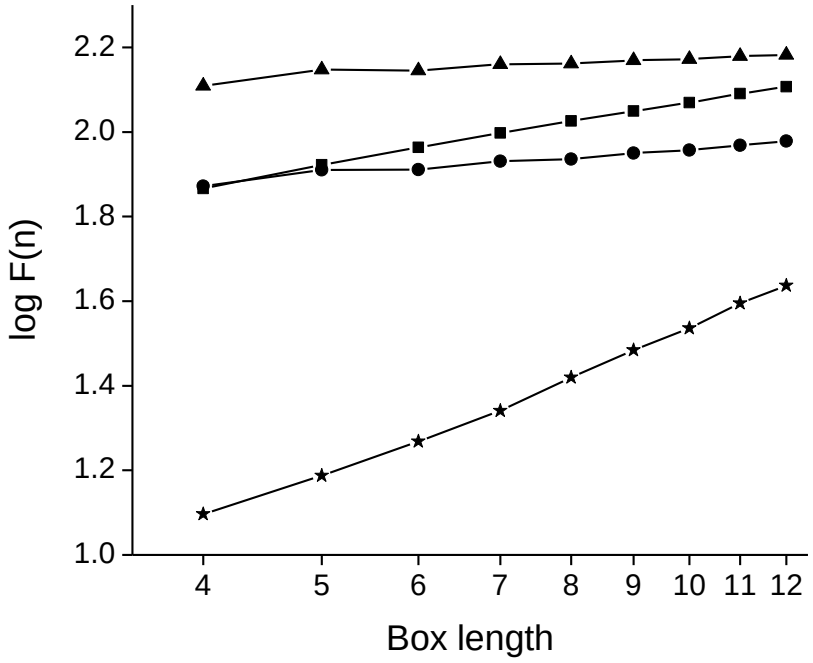

Figure 2.5 Relationship between the fluctuations function F(*n*) and the box size *n* in a double logarithmic plot. Shapes to the four different RR interval segments: stars corresponds to NSR, squares to AF, triangles to SR with PVCs and filled circles to SR with PACs.

To explain these results, we refer to Figure 2.4: open circles represent the integrated time series, the red and green lines indicates the linear interpolation for box size *n*=4 and *n*=12, respectively. Looking at the distance between the circles and the red line, it is clear how F(*n*) for box length equal to 4 differs among the groups: NSR (*a*) has the lowest value, AF (*b*), SR with PVCs (*c*) and PACs (*d*) larger values. As the scale *n* increases, a concomitant increase of F(*n*) is appreciable in all the 4 groups – looking at the distance between the circles and the green lines, even if with very different magnitude. For NSR the increment is elevated, and this is reflected by the highest value of the slope, for AF it is still significant but lower than NSR, and the slope, consequently, has a reduced value. In the cases of SR with ectopic beats the increase is very little, generating almost flat lines in the log-log plot; the scaling exponents are indeed the lowest.

LDs is computed on the averaged histogram of template count as a function of template matches calculated every 12 beats. Figure 2.6 illustrates the step-by-step procedure in a 12-beat segment extracted from the same 30-second record of Figure 2.3 (gray filled circles). Two points are considered: the half-filled square, in Figure 2.6(*a*), has 2 matches (crosses), whereas the filled square, in Figure 2.6*(b*), counts 8 matches within a tolerance of 20 msec. The contribution of each of the two interbeat intervals to the histogram is highlighted in Figure 2.6(*c*). Repeating this counting for all the 12 points, the final histogram of the templates counts as a function of the number of matches is obtained.

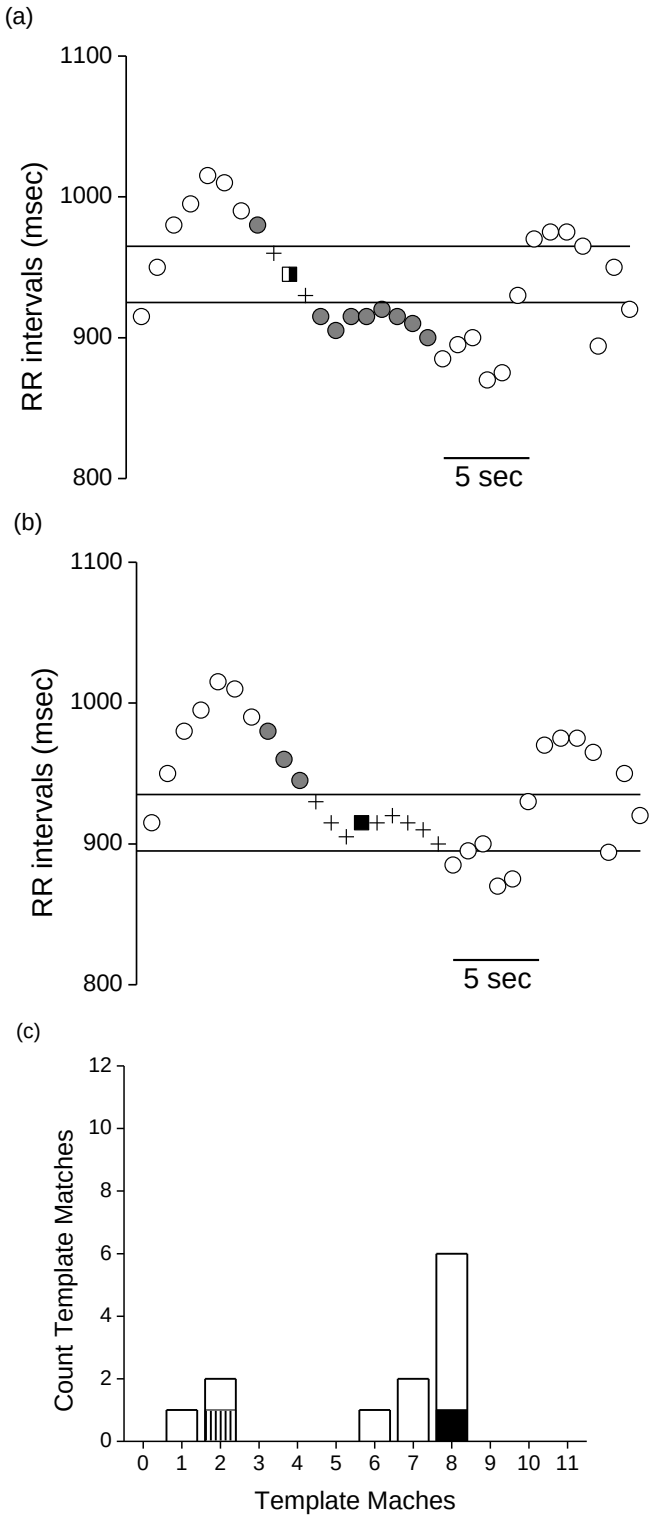

Figure 2.6 Illustration of the calculation of the LD histogram for a 12-beat segment extracted from 30-second record of a healthy patient of the UVa Holter database. The half-filled square and the filled square are the samples taken into account for the calculation of matches respectively in (*a*) and (*b*) panels on the same 12 beat segment. The crosses represent the matches within a tolerance of 20 msec. (*c*) LD histogram based on the count of templates as a function of the number of matches. The remaining sample of the 12-beat segment are represented by the grey circles. The half-filled square sample has 2 matches, the filled square sample has 8 matches, and therefore they contribute to the bin 2 and 8 respectively.

The average histograms for the 10-minute segments represented in Figure 2.2 are shown in Figure 2.7. As expected, in AF condition most templates find very few matches (Figure 2.7 (*b*)), whereas a bell-shape histogram distribution was obtained for the NSR series (Figure 2.7 (*a*)). In case of PVCs the histogram is similar to the AF case, due to the high amount of ventricular ectopic beats which produces high values in the first bins of the histogram (Figure 2.7 (*c*)). For SR with PACs (Figure 2.7 (*d*)), the histogram reports a peak in correspondence of bin 5 and the majority of templates finds a number of matches less than 5. Intuitively, the peak appears due to the alternation of accelerated and delayed beats, associated to the bigeminy.

LDs is computed on the histograms. The highest score of 2.05 belongs to AF, as expected, followed by SR with PVCs (LDs = 1.24), due to its high burden of ectopy. NSR and SR with PACs both have a low score, equal to 0.28 and 0.54, respectively. This is expected in the case of NSR, due to its distribution mainly concentrated in the center of the histogram, while in the case of SR with PACs the low value is related to the specific pattern of bigeminy, which corresponds to low counts in bins 0, 10 and 11.

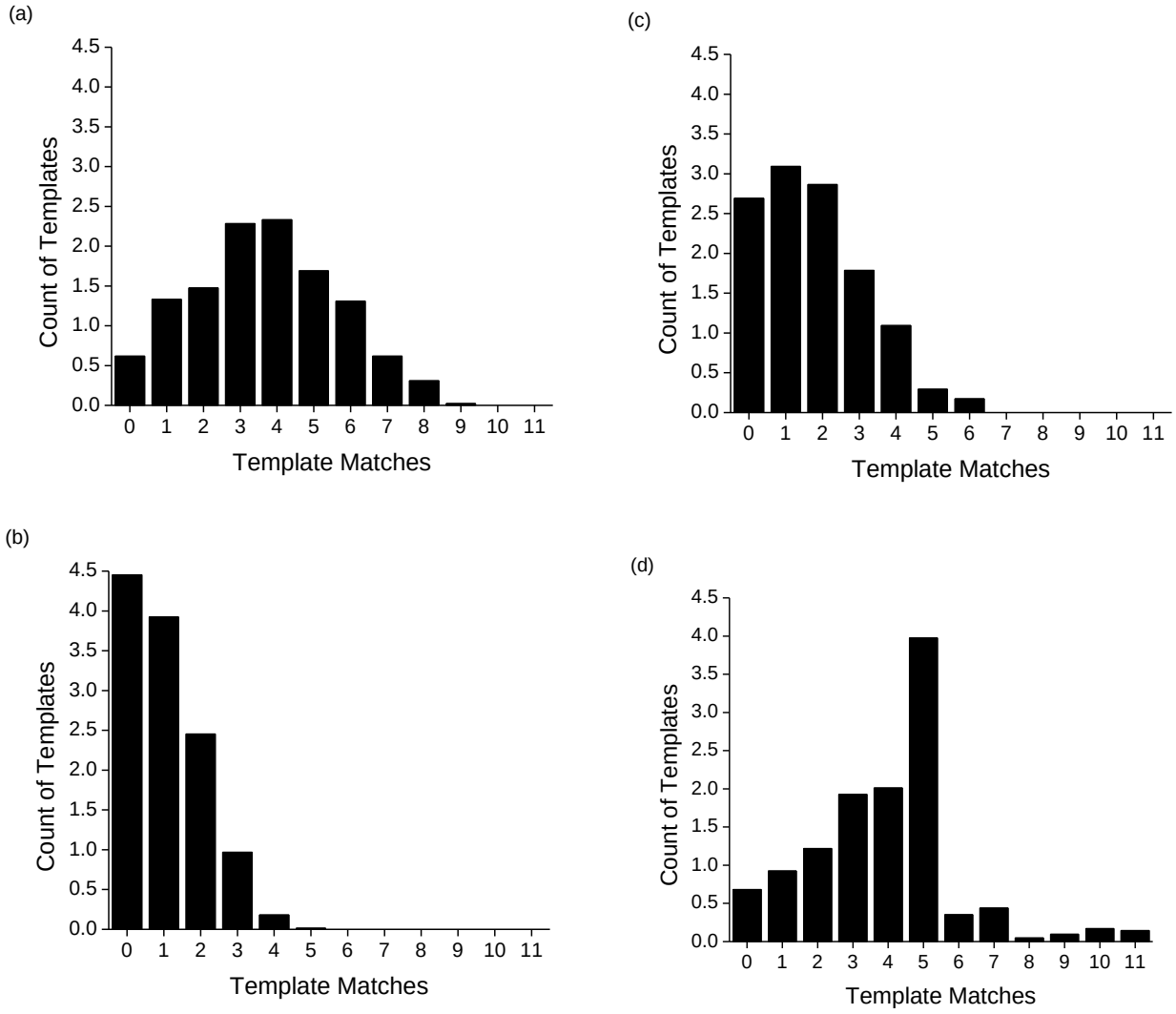

Figure 2.7 Average histograms of the count of templates as a function of the number of matches for the 10-minute RR interval time series displayed in Figure 2.2.

We further investigated the effect of ectopy on dynamical measure. Figure 2.8 shows the distribution of each index as a function of the burden of ectopy calculated on all 10-minute records, with the 95% confidence interval. The bins in the figure are constructed after ranking the sequences according to ectopy burden, and by setting the bins distance equal to a fixed percentile increment, i.e. 2%. As expected, ectopic beats increase entropy and the related LDs – after a point - though, entropy falls with increased ectopy. This may be caused by the particular arrhythmias named trigeminal and bigeminal rhythms, or non-sustained atrial and ventricular tachycardia. The regularity of these abnormal rhythms accounts for the lower entropy values. The fall in DFA slope reflects the effects of ectopic beats on the dynamics of the RR interval time series. The physiological condition (NSR) is characterized by long-range correlations, the presence of ectopic beats plays a role such as an uncorrelated noise. As resulting effect the slope values falls below 0.5.

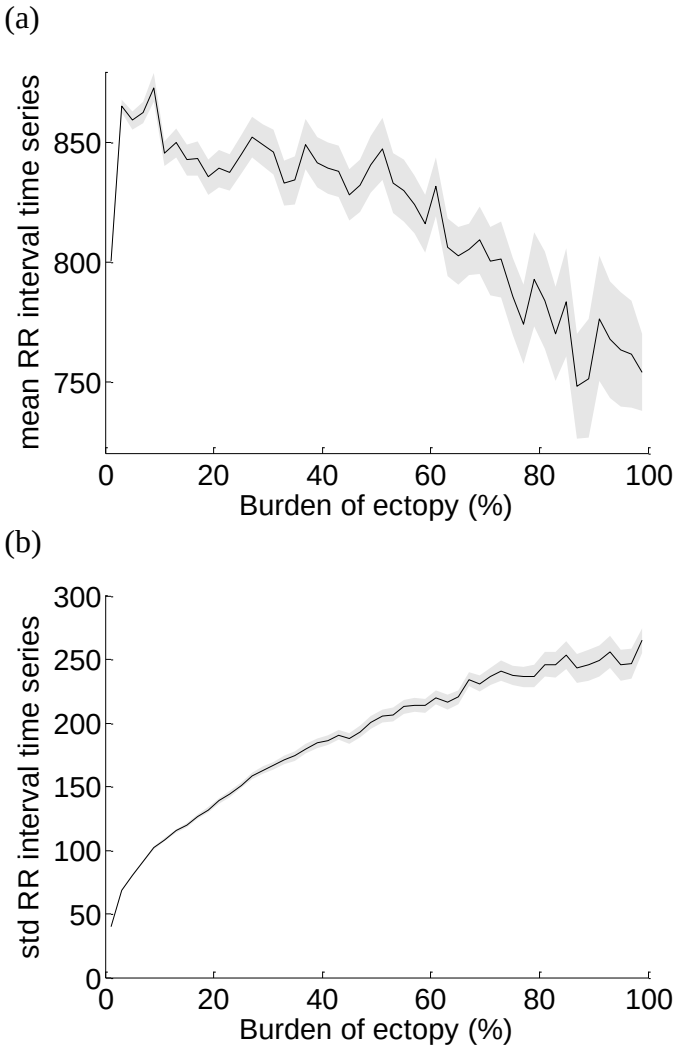

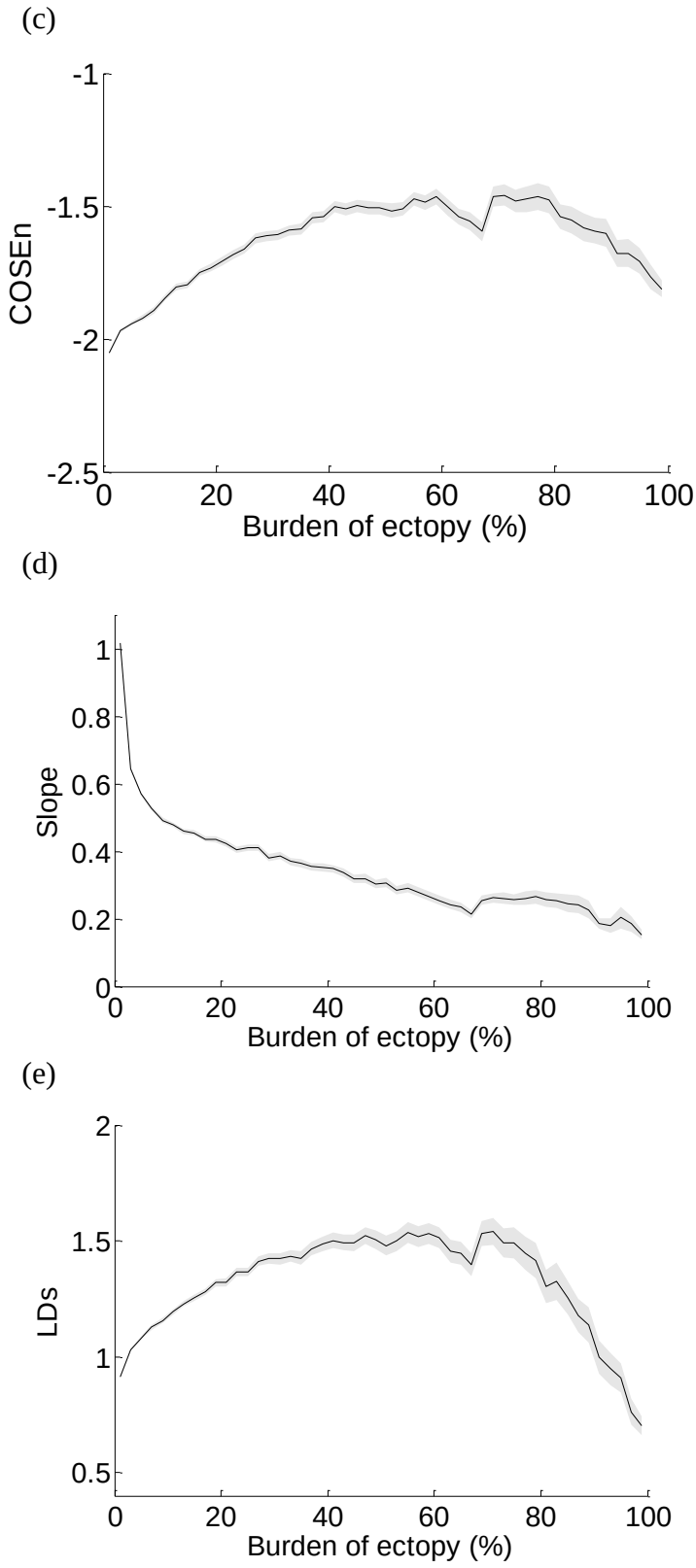

Figure 2.8 Mean (*a*) and standard deviation (*b*) of the RR intervals time series, COSEn (*c*), scaling exponent (slope) (*d*) and LDs (*e*) as a function of the burden of ectopy. In black the average trend. The gray region indicates the 95% confidence intervals.

2.5.2 Univariate analysis

Table 2.1 presents the median and (25°,75°) percentile values for each group and for each parameter discussed in the previous paragraphs. Significant differences were obtained for all the parameters except for mean and the standard deviations of RR interval time series, using Kruskal-Wallis test. As expected, NSR had the lowest variability (Std), entropy and LDs, and the highest DFA values.

Table 2.1 Median and (25°,75°) percentile values of the parameters for each group

Parameters	*AF*	*NSR*	*SR with ectopy*	*Kruskal-Wallis test p-value*
Mean RR (sec)	763 (660,884)[b]	795 (676,928)[b]	820 (707,942)	< 0.001
Std RR (sec^2)	149 (116,186)	38 (24,58)[a,b]	152 (108,208)	< 0.001
COSEn	-0.5 (-0.8,-0.3)[b]	-2.1 (-2.3,-1.8)[a,b]	-1.7(-2,-1.4)	< 0.001
LDs	1.92 (1.5,2.36)[b]	0.84 (0.52,1.33)[a,b]	1.28 (1.01,1.62)	< 0.001
DFA	0.61 (0.56,0.66)[b]	0.98 (0.66,1.26)[a,b]	0.32 (0.21,0.5)	< 0.001
Age	71.9 (64.9,78.8)[b]	47 (22.5,65.6)[a,b]	58.4 (20.1,73.5)	< 0.001

Post-hoc comparisons p-value <0.05: [a] vs. AF, [b] vs. SR with ectopy

2.5.3 Logistic regression analysis

The strategy of classification was based on three multivariate logistic regression models, each used to discriminate one group from the other two. This parametric analysis hypothesized a linear relationship among the effects of the independent predictor variables on the predicted output.

Table 2.2 shows the accuracy of labeling 10-minute records using the standard factors model in the test set. The columns give the correct classification based on the labels provided by the software. The rows show the classification results from the model adopted. The numbers in the table were obtained from the average of the results of the 10-folds cross-validation procedure. The accuracy is 88.4% and the positive predictive values, reported in the last column of the table, are 63%, 92% and 62% for AF, NSR and SR with ectopy, respectively.

Table 2.2 Contingency matrix of Multi-label model with linear measures and Positive Predictive Values

	AF	**NSR**	**SR with ectopy**	**PPV**
AF	984.5 (34%)	85.6 (0%)	496.2 (10%)	63%
NSR	373.3 (13%)	29333.4 (99%)	1559.7 (31%)	92%
SR with ectopy	1618.4 (53%)	223.8 (1%)	3053.6 (60%)	62%

Table 2.3 shows the accuracy of labeling 10-minute records considering the second model, when also non-linear indices are taken into account. The accuracy of the classification rises to 94.1% and the positive predictive values, reported in the last column of the table, becomes 89%, 96% and 86%.

Table 2.3 Contingency matrix of Multi-label model with dynamical measures and Positive Predictive Values

	AF	NSR	SR with ectopy	PPV
AF	2377.8 (81%)	77.1 (0%)	213.7 (4%)	89%
NSR	317.9 (10%)	29179.8 (99%)	962.9 (19%)	96%
SR with ectopy	280.5 (9%)	385.9 (1%)	3932.9 (77%)	86%

A fixed threshold to classify a segment as NSR or SR with ectopy was chosen equal to 10%, reflecting clinical practice. However, one of the most common errors of this system is when SR has little amount of ectopy, which are the main causes of misleading with NSR. We further tested the accuracy of the new model by varying the threshold from 4% to 20% with an increasing step of 2%. An improvement of the exact match of segments classified as SR with ectopy was obtained from a value of 55% (4% burden) to 89% (20% burden), while NSR accuracy decreases of about 2%. The overall accuracy rose from 88.9% to 93.7% and peaked at 94.4% in correspondence of a threshold of 14% burden.

For a further discrimination between SR with PVCs or PACs, we tested a new strategy of classification with four logistic regression models. The final decision classified the RR interval time series by using the highest output among the four models. Table 2.4 shows the results. An accurate differentiation of the two situations of ectopy is not feasible: low accuracies are associated with the two classes of ectopy, with a big misclassification of SR with PVCs as SR with PACs (44%) and high percentages of misleading with NSR. Moreover, the value of 13% of error between SR with PACs and AF model shows that the two arrhythmias are easily confused, a situation that can be reasonably expected. Positive predictive accuracies are equal to 85%, 94%, 65% and 58%, for AF, NSR, SR with PVCs and PACs, respectively. When considering the two classes of ectopy together in a three-based models scheme, the positive predictive accuracy rises to 85.5%. These findings confirm that the best classification strategy is the one based on three classes.

Table 2.4 Contingency matrix of Multi-label model with four groups

	AF	NSR	SR with PVCs	SR with PACs	PPV
AF	2471.4 (83%)	86.4(0%)	96.9 (3%)	265 (13%)	85%
NSR	353.3 (12%)	29358.1 (99%)	783.3 (26%)	605.6 (30%)	94%
SR with PVCs	95.2 (3%)	169.3 (1%)	2099.5 (67%)	882.4 (44%)	65%
SR with PACs	56.3 (2%)	29 (0%)	110.8 (4%)	266 (13%)	58%

2.5.4 k-Nearest Neighbor analysis (k-NN analysis)

This analysis requires no apriori model, because it belongs to the nonparametric clustering methods category. For the k-NN analysis a first selection of the optimal parameters was necessary, in particular, the metric for calculating the distance between the current query point and the training set, and the number of neighbors (K). We analyzed three distance metrics: the Euclidean distance, the standardized Euclidean distance and the Mahalanobis distance. Their efficiency was tested on the same dataset using a 10-fold cross-validation procedure with an initial value of K = 1. The strategy was to classify a 10-minute segment based on the classification of the majority of its neighbors. For a new test record x_i, distances from all the points of the training set are sorted in ascending order. Fixed the number K of neighbors, the first K smallest distances are chosen and their classes are taken into account for the final decision: the new record is assigned a probability to be in one of the three classes and the higher value was selected for the classification. The overall accuracy of the classification with the three approaches, i.e. Euclidean distance, standardized Euclidean distance and Mahalanobis distance, was 87.9%, 92.8% and 92.7%, respectively. The standardized Euclidean distance was selected for further investigations. The accuracy of the classifier with the chosen distance metrics was tested as a function of the number of neighbors K. It rises for small K, but for numbers greater than 15 the value remains constant, at approximately 94.55%. We chose K=25 for the successive analyses.

Table 2.5 and Table 2.6 report the accuracy obtained with the k-NN classifier of labeling 10-minute records using the minimal model with the standard indices (i.e. with the mean and SD of RR intervals time series) and the new model, respectively. The overall accuracy is 89.4% in the first case and equal to 94.5% in the second case. Positive predictive values are 90%, 97% and 84% for AF, NSR and SR with ectopy, respectively.

Table 2.5 Contingency matrix of k-NN model with linear measures and Positive Predictive Values

	AF	**NSR**	**SR with ectopy**	**PPV**
AF	1589.4 (54%)	95.4 (0%)	976.9(20%)	60%
NSR	266 (9%)	28210.7 (98%)	930.3 (19%)	96%
SR with ectopy	1077.3 (37%)	532.5 (2%)	3056.4 (61%)	66%

Table 2.6 Contingency matrix of k-NN model with dynamical measures and Positive Predictive Values

	AF	**NSR**	**SR with ectopy**	**PPV**
AF	2388.4 (82%)	72.4 (0%)	201.4 (4%)	90%
NSR	266 (9%)	28265.2 (98%)	683.1 (14%)	97%
SR with ectopy	278.3 (9%)	501(2%)	4079.1 (82%)	84%

2.5.5 Validation on a different database

The proposed classifiers are also externally validated on the canonical MIT-BIH database, which includes the AF, NSR and other arrhythmias (ARH) databases (Goldberger et al, 2000). The MIT-BIH AF database consists of 10-hour recordings from 25 patients with AF with 1.22 millions of RR intervals, 42.5% labeled as AF. The ARH database consists of 30-minute recordings from 48 patients with various arrhythmias with 0.1 millions of RR intervals, 11% labeled as AF. The NSR database consists of 24-hour recordings from 72 patients with a total of 7.52 millions of RR intervals, some of them labeled as ectopy but none labeled as AF. In all, there are 11'290 10-minute segments in the combined data sets, 644 that we labeled as AF. This 6% prevalence of AF is similar to the 10% in the UVa Holter data set. In contrast, though, is the small number of 10-minute segments with 10% or more ectopic beats – only 94 (0.8%).

As external validation, we tested the regression-based scheme and the k-NN algorithm on the individual (Tables *a, b, c*) and combined (Tables *d*) MIT-BIH data sets divided into 10-minute segments. Table 2.7 and Table 2.8 show the results of the rhythm classifications achieved by the regression-based schemes and k-NN, respectively.

The results obtained of accuracies and positive predictive values in case of AF and NSR in the combined databases (Table 2.7d and Table 2.8d) are higher than those found for the UVa Holter database. However, for what concern SR with ectopy, the values are lower. We think that this is due to the low prevalence of SR with ectopy segments, which is only 0.8%, as already discussed previously.

We observed a problem in performing the k-NN algorithm on the combined databases related to the lack of age information for some patients. While in computing the logistic regression based scheme an appropriate model was created if the data of age was missing, in the case of the non-parametric k-NN method it was not possible and we discarded the age values from the analysis on the combined databases. We can reasonably assume, though, that the results would have been better if the age was included.

Table 2.7a Logistic Regression analysis on MIT-BIH AF database

	AF	NSR	PPV
AF	485 (77%)	8 (1%)	98%
NSR	92 (15%)	713 (87%)	89%
SR with ectopy	49 (8%)	94 (12%)	0%

Table 2.7b Logistic Regression analysis on MIT-BIH ARH database

	AF	NSR	SR with ectopy	PPV
AF	14 (78%)	0 (0%)	5 (17%)	74%
NSR	3 (16%)	56 (97%)	3 (10%)	90%
SR with ectopy	1 (6%)	2 (3%)	21 (73%)	88%

Table 2.7c Logistic Regression analysis on MIT- BIH NSR database

	AF	NSR	SR with ectopy	PPV
AF	0	8 (0%)	1 (2%)	0%
NSR	0	9631 (100%)	7 (11%)	100%
SR with ectopy	0	40 (0%)	57 (88%)	59%

Table 2.7d Logistic Regression analysis on all 3 combined MIT database

	AF	NSR	SR with ectopy	PPV
AF	499 (77%)	16(0%)	6 (6%)	96%
NSR	95 (15%)	10400 (100%)	10 (11%)	99%
SR with ectopy	50 (8%)	42 (0%)	78 (83%)	40%

Table 2.8a k-NN analysis on MIT- BIH AF database

	AF	NSR	PPV
AF	514 (82%)	13 (2%)	98%
NSR	63 (10%)	688 (84%)	92%
SR with ectopy	49 (8%)	114 (14%)	0%

Table 2.8b k-NN analysis on MIT- BIH ARH database

	AF	NSR	SR with ectopy	PPV
AF	14 (78%)	0 (0%)	1 (4%)	93%
NSR	2 (11%)	56 (97%)	3 (10%)	92%
SR with ectopy	2 (11%)	2 (3%)	25 (86%)	86%

Table 2.8c k-NN analysis on MIT- BIH NSR database

	AF	NSR	SR with ectopy	PPV
AF	0	25 (0%)	1 (1%)	0%
NSR	0	9588 (99%)	1 (1%)	100%
SR with ectopy	0	66 (1%)	63 (98%)	49%

Table 2.8d k-NN analysis on all 3 combined MIT databases (without age)

	AF	NSR	SR with ectopy	PPV
AF	528 (82%)	15 (0%)	0 (0%)	97%
NSR	66 (10%)	10366 (99%)	5 (5%)	99%
SR with ectopy	50 (8%)	57 (1%)	89 (95%)	45%

Chapter 3

2-years mortality risk analysis based on heart rate dynamics

3.1 Introduction

Abnormal dynamics of heart rhythm are associated with an increased risk of mortality. As already discussed in §1.3, AF and situations of normal variability punctuated with atrial or ventricular ectopy are strongly associated with an increased risk of mortality. AF is generally accepted as one of the most important risk factors for stroke (Wolf et al, 1991) and it is associated to other cardiac diseases, such as tachycardia-induced cardiomyopathy, congestive heart failure and valve disease (Stewart et al, 2002). Many studies have been presented in order to assess the independency of AF as a risk factor for mortality, but if this is a direct effect of AF itself or is related to the risky conditions associated with it, is still under study (Leong et al, 2013). Ventricular ectopy have been thought for a long time to be benign when occurring in healthy hearts, but recent studies shed light on the evidence of poor prognosis associated with PVCs, even in hearts with no structural diseases (Cha et al, 2012) (Lee et al, 2012). There are proofs that PVCs may lead to adverse prognosis by generating fatal arrhythmias and heart failure. PVC-induced cardiomyopathy and left ventricular dysfunction can be reversed by radiofrequency ablation, and studies demonstrated that the ejection fraction rises at the time of PVC ablation (Yokokawa et al, 2013). Premature atrial contraction are known to precede AF (Haissaguerre et al, 1998) and to be surrogate markers of paroxysmal AF in patients with acute ischemic stroke (Wallmann et al, 2007).

Specific parameters to detect abnormalities in the cardiac rhythm have been already developed. The coefficient of sample entropy was optimized for AF detection, while the local dynamics score was specifically designed to recognize the

abnormal dynamic phenotype associated with reduced variability and occurrence of ventricular ectopy.

In this work, a mortality risk stratification analysis was performed on the University of Virginia (UVa) Holter database, and we show how, combining these two heart rate dynamical measures, a picture of mortality risk can be obtained.

3.2 Study population

The analysis was performed on 1’518 RR interval time series from a database of 2’440 ambulatory patients that were prescribed for 24-hour Holter monitoring at the Health System Heart Station, University of Virginia (UVa), USA, from 12/2004 to 10/2010. Only patients with age over 40 were taken into account based on the low incidence of AF in younger patients, thus the dataset shows an overall average value of 65±13 years. The mortality rate in two years was 5%. We used Philips Holter Software labels of AF, premature atrial and ventricular beats. The recordings were classified as previously described in §2.2, by taking a fixed threshold of 10% burden for ectopic beats. The dataset is composed of 71% NSR, 13% AF and 15% SR with ectopy recordings.

3.3 Methods

COSEn is a measure derived from the sample entropy and it is developed specifically for the detection of AF in very short RR interval time series (Lake and Moorman, 2011). For the details of its calculation we refer to §2.3.1. In this study COSEn was assessed on 30 second segments and we averaged all results over 24 hours. For those recordings with an AF burden lower than 90%, we analyzed only the segments where each beat was labeled as AF.

LDs is a new index to investigate the local dynamics of short time series and the overall calculation is explained in § 2.3.3. The prognostic importance of this index has been evaluated by Moss et al (2014), who introduced LDs as a significant independent predictor factor of mortality in ambulatory patient undergoing 24hr Holter, in addition to standard risk factors such as age, hypertension, diabetes, hyperlipidemia, history of tobacco use and history of congestive heart failure (Moss

et al, 2014). Results show that patients with higher local abnormalities, i.e. higher values of the index, were subject to higher mortality during a follow-up of 8 years. High values can be reached with both situations of high irregularity, such as AF or ectopy, or very low variability, such as conditions of reduced heart rate variability. For what concern the LDs calculation, we averaged the result of the number of templates as a function of the number of matches from all 12-beat segments in 24 hours and we assessed the score on the average histogram.

To analyze the distribution of the population and its relative mortality risk as a function of COSEn and LDs, we performed a multivariate kernel density study on the histograms of the joint distributions of the parameters. The multivariate kernel density approach helps in solving the problem related to the estimation of probability density functions. In a case of bivariate analysis, the estimation consists in constructing the histograms and creating a map of the dataset where the density is assigned with the use of a grid, whose dimensions are based on the bin width of the univariate histograms. This approach has the disadvantage to be affected by the bins size and by the grid starting point. However, the use of kernel functions creates a density map smoothed out from every single data point into its surrounding region of space, obtaining a smoother result and a performance not dependent on the width of histogram's bins.

In this study the kernel chosen is a bivariate Gaussian with a diagonal bandwidth matrix, which allows different amounts of smoothing in each of the coordinates (Botev et al, 2010). Because of the choice of the bandwidth matrix is the most important factor affecting the accuracy of the estimation, since it controls the orientation and the amount of smoothing induced, the two bandwidth parameters are chosen optimally without assuming a parametric model for the data (Lake, 2009).

3.4 Results

Color maps of the joint distributions of COSEn and LDs are shown in Figure 3.1 for different groups of population. Panel (*a*) shows the entire database, panel (*b*) all the patients who died within two years, panel (*c*) all the survivals and, finally, panel (*d*) illustrates a color map of 2-years mortality risk, which is computed as the ratio of the joint distributions of COSEn and LDs of the patients who died and the whole population. The majority of the patients survived and has low values of COSEn and LDs, as demonstrated by the high density regions in panels (*a*) and (*c*). About 5% of the population died and these are patients characterized by higher values of both the indices. A scatter plot of the dead people over the survival is reported in Figure 3.2, to quantitatively assess the previous results discussed. These findings are summarized in panel (*d*) showing the mortality risk. The color bar defines the different levels of mortality risk. The light blue, i.e. the color associated with the value 1, indicates regions that have a risk equal to the average mortality rate of the dataset. Cooler colors indicate areas associated with a lower risk, whereas regions marked with warmer colors denote higher risk. For example, patients in regions with a color value of 0.5 have a mortality risk equal to half of the average, whereas orange regions hold patients with a 2 times higher risk than the average.

A well-defined royal blue region, i.e. with very low mortality risk, is characterized by low values of LDs, whereas high-risk zones are related to higher values of the index. A mutual increase of LDs values and mortality risk is thus observable. In particular, starting from the low risk region (left lower edge), it is possible to distinguish two different directions along which the risk becomes higher: the first, marked by the lower arrow, evolves toward increased values of LDs independently of COSEn values, whereas the second one, highlighted by the upper arrow, points toward both higher values of LDs and COSEn, reaching the maximum for both the indices.

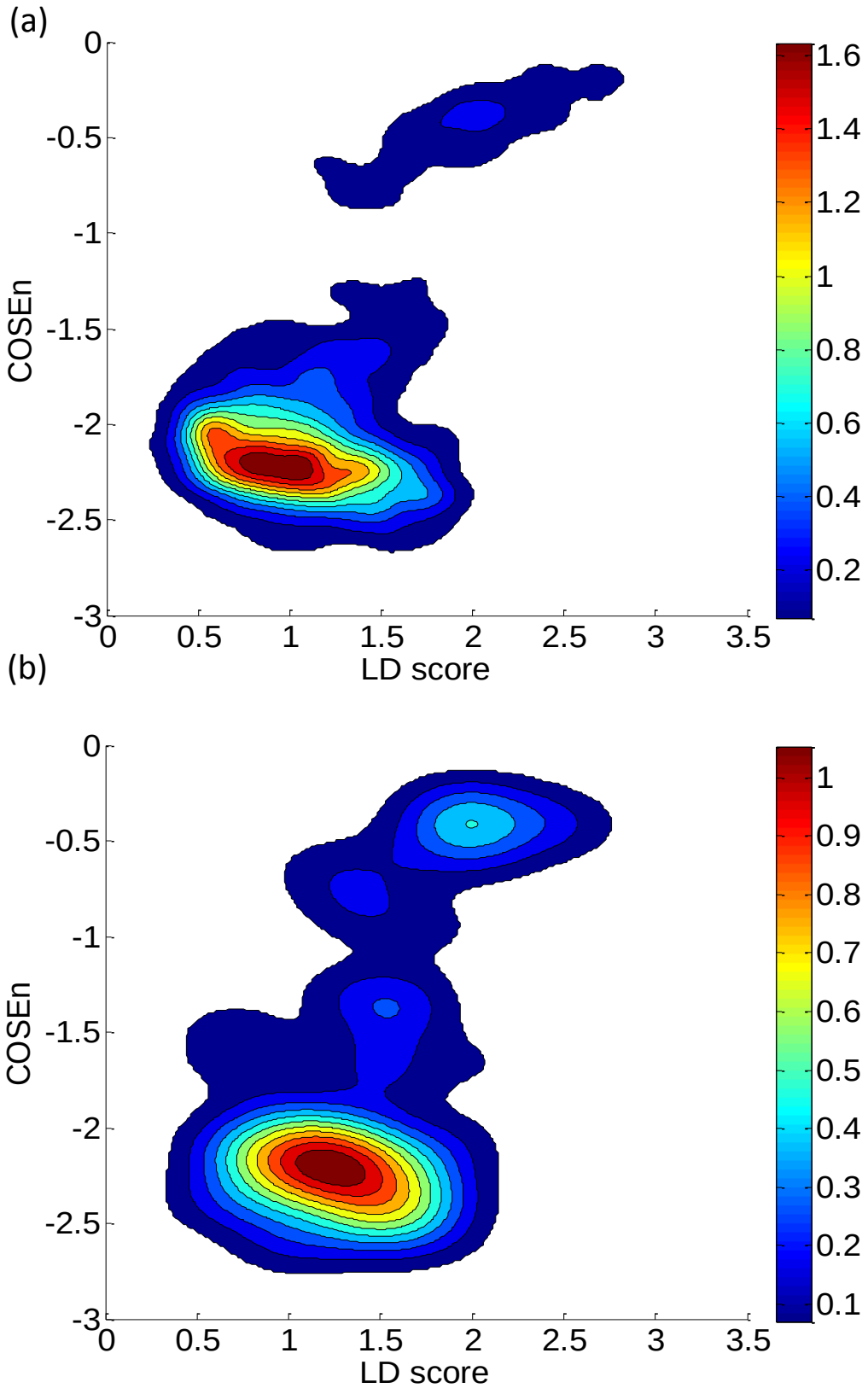
(a)
COSEn
LD score
0
-0.5
-1
-1.5
-2
-2.5
-3
0
0.5
1
1.5
2
2.5
3
3.5
1.6
1.4
1.2
1
0.8
0.6
0.4
0.2
(b)
COSEn
LD score
0
-0.5
-1
-1.5
-2
-2.5
-3
0
0.5
1
1.5
2
2.5
3
3.5
1
0.9
0.8
0.7
0.6
0.5
0.4
0.3
0.2
0.1

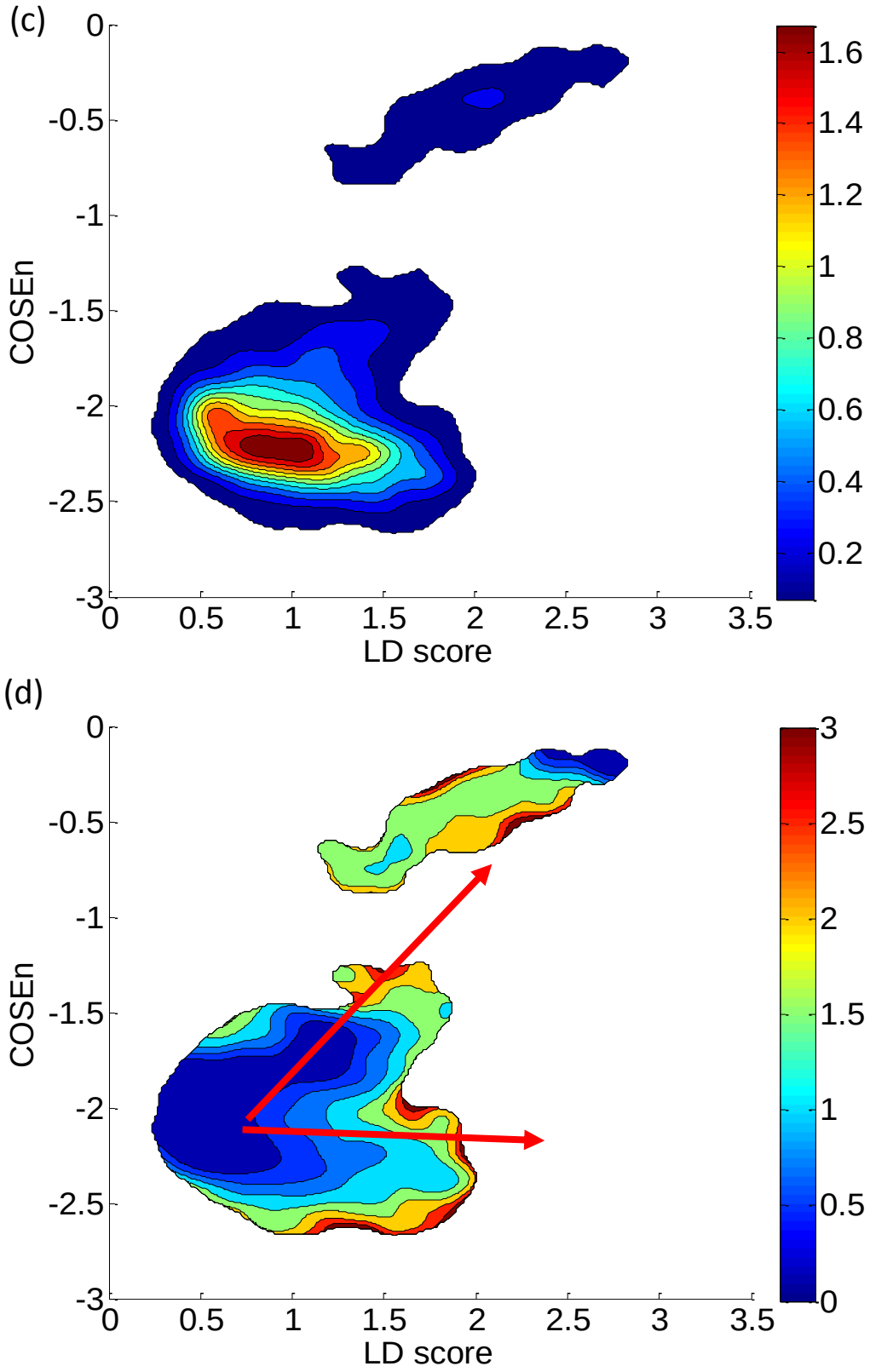

Figure 3.1 Color maps of the joint distributions of COSEn and LDs for different groups in the UVa Holter population. Panel (*a*) shows all the patients, panel (*b*) shows the patients who died within two years, panel (*c*) shows all the survivals and panel (*d*) the mortality risk over two years. The color bar indicates the fold-increased risk. The arrows in panel (*d*) mark the directions towards increasing risk from a region of very low risk to areas with higher risk.

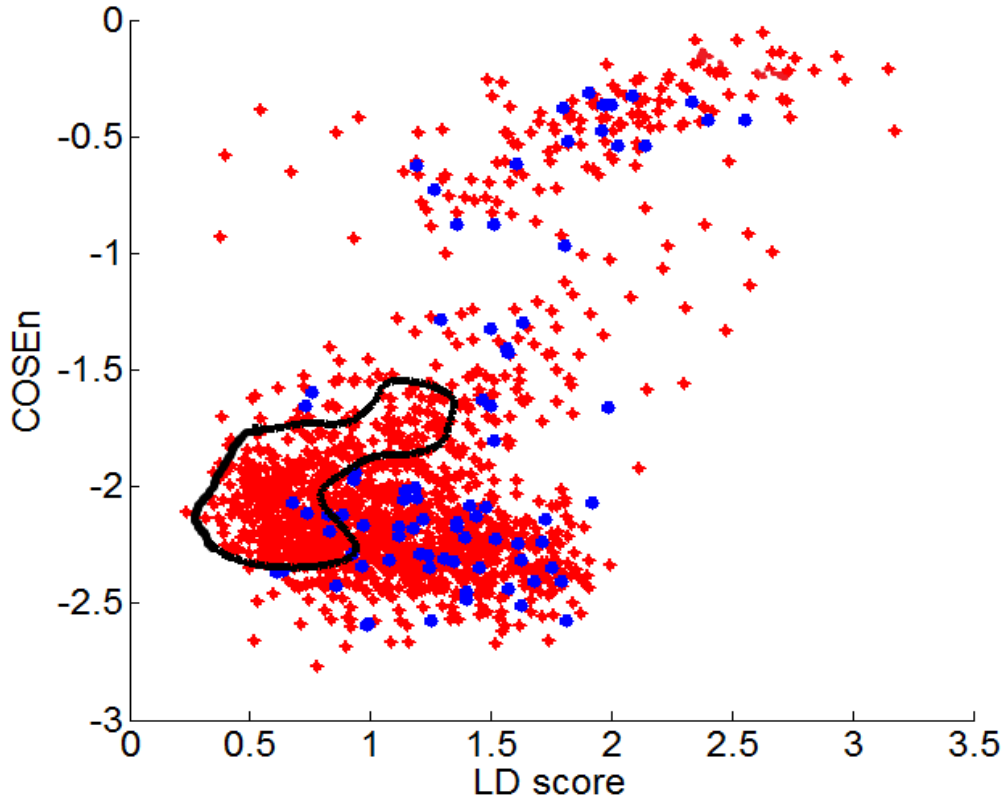

Figure 3.2 Distribution of the average values over 24 hours of LDs and COSEn for the UVa Holter population. Red dots mark the patients who survived, blue dots the patients who died within two years. The black line indicates the low risk region represented with royal blue color in Figure 3.1(*d*).

Figure 3.3 shows the distribution of the 24-hour average values of LDs and COSEn for the population. The three groups AF, SR with ectopy and NSR are labeled by their colors. The red dots represent the AF patients: it is noticeable that the majority of them has the highest values of COSEn and LDS, and that they are gathered in an upper corner almost separated from all the rest of the population. Blue dots denote patients in NSR, which have the lowest averaged value of COSEn, but they are scattered over a wide range of LDs values, from 0.5 to 2. Finally the patients in SR with ectopy denoted by green dots, have intermediate values of both COSEn and LDs. The AF group had higher mortality. This is expected, given its increased occurrence in patients with heart disease.

The arrows of Figure 3.1(*d*) draw attention to two trends of heart rate dynamics in higher-risk patients. The lower arrow follows a group with high LDs and low COSEn: looking at the

Figure 3.3, these are patients with SR with reduced variability and little or no ectopy. The upper arrow follows a group with high LDs and intermediate COSEn, not high enough to signify AF: these patients have SR and a high burden of ectopy.

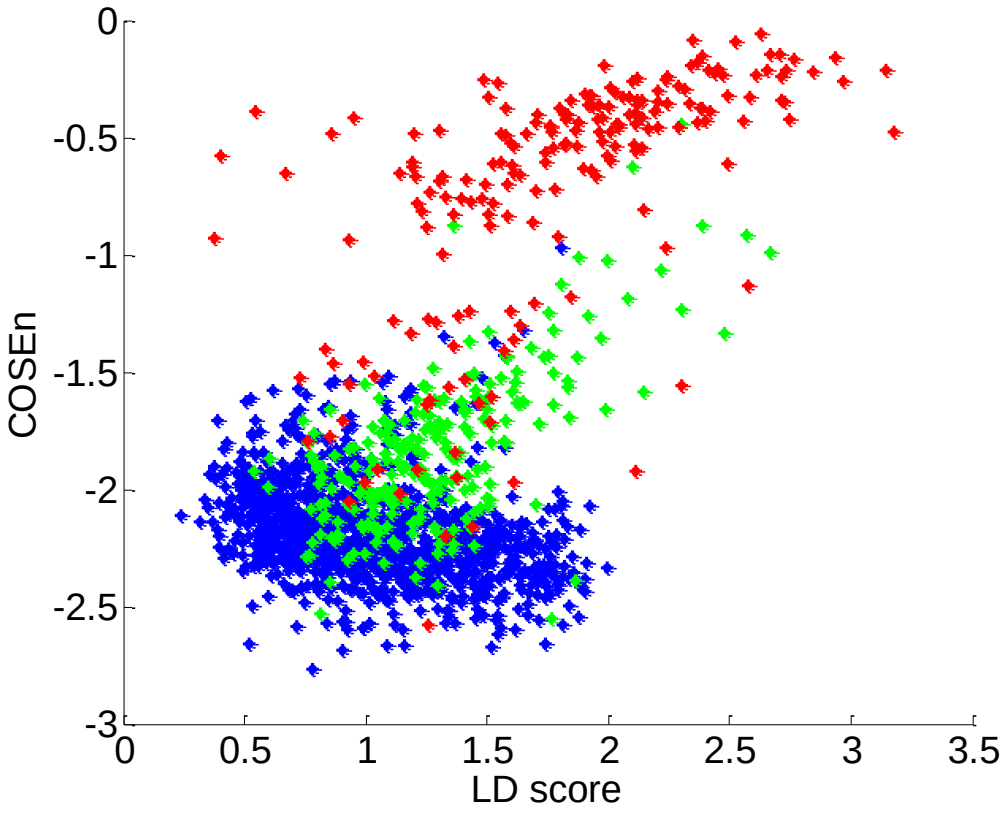

Figure 3.3 Distribution of the average values over 24 hours of LDs and COSEn for the UVa Holter population. The three categories of AF, NSR and SR with ectopy are displayed with different colors: red for AF, blue for NSR, green for SR with ectopy.

An example of 24-hour recording of four patients with different heart rhythm is presented in Figure 3.4, with features of NSR (*a*), SR with ectopy (*b*), AF (*c*) and SR with low variability (*d*).

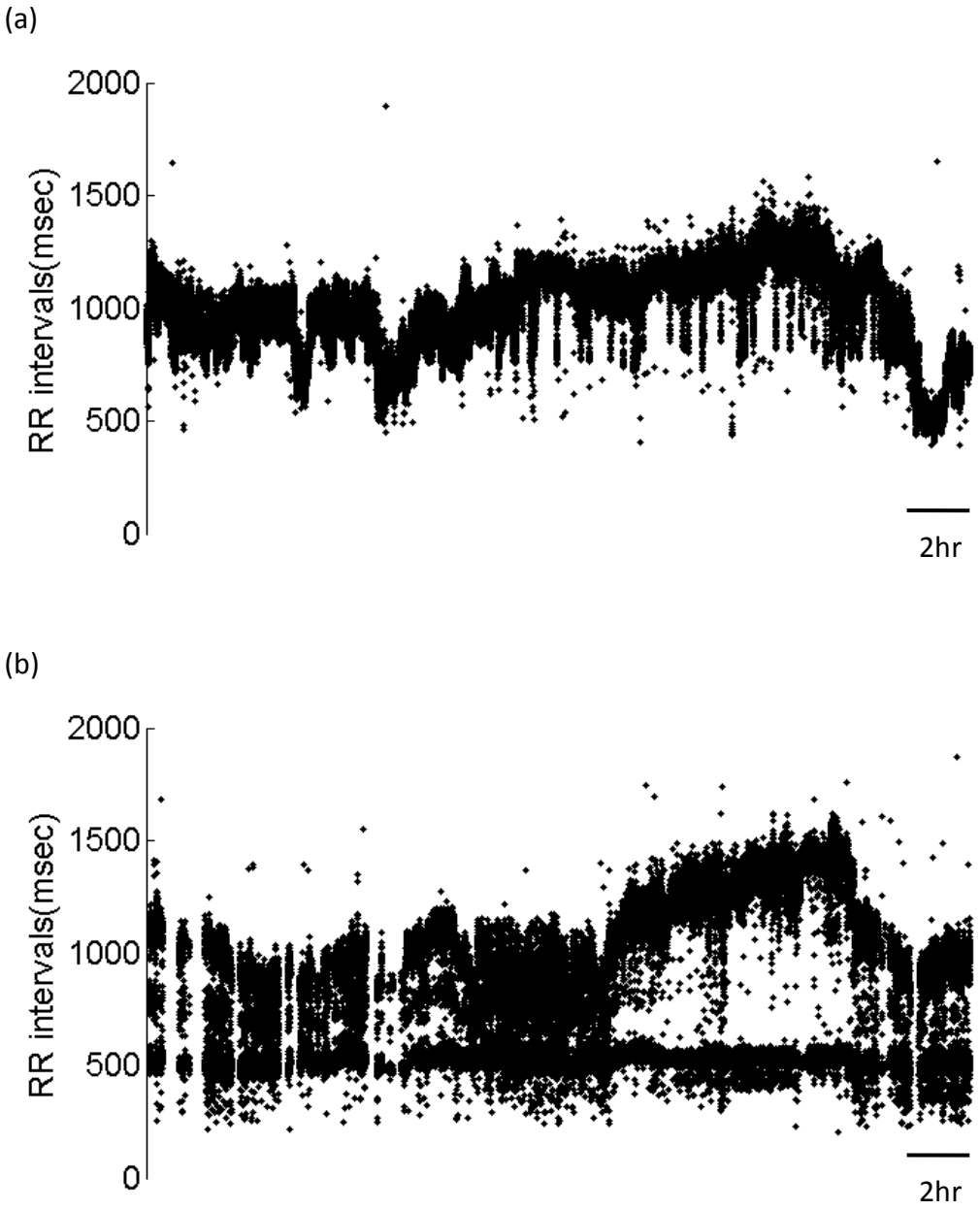

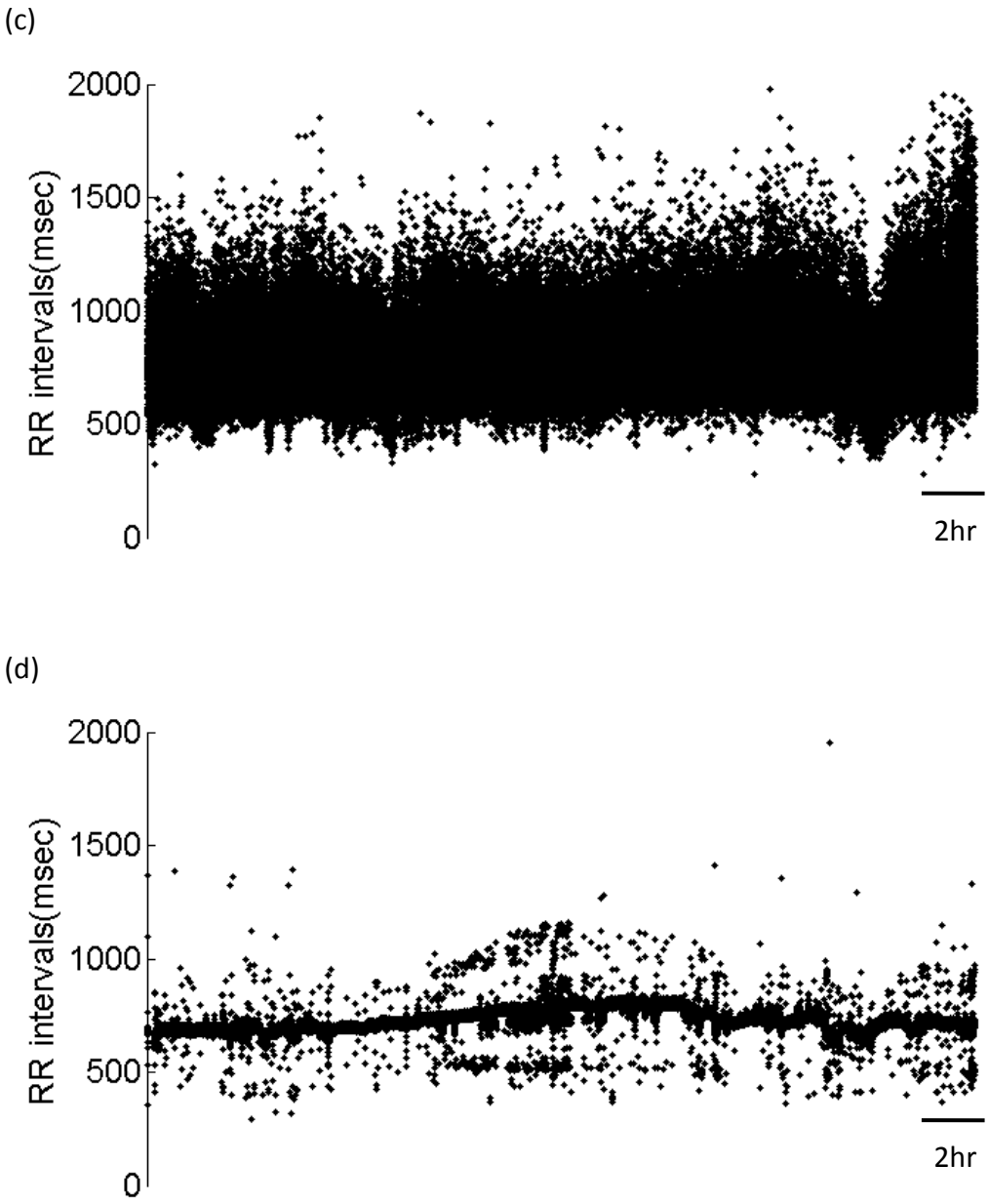

Figure 3.4 RR interval time series of 24 hours from the UVa Holter database for NSR (*a*), SR with ectopy (*b*), AF (*c*) and SR with reduced variability (*d*).

Interestingly, we do not find large differences in the dynamics of atrial and ventricular ectopy, as Figure 3.4 shows with a clear overlap between the two classes. This is clinically counter-intuitive, as the coupling intervals of PVCs are perceived to be more regular than those of PACs. No direct comparisons of the dynamics of atrial and ventricular ectopy are currently available to shed light on this issue.

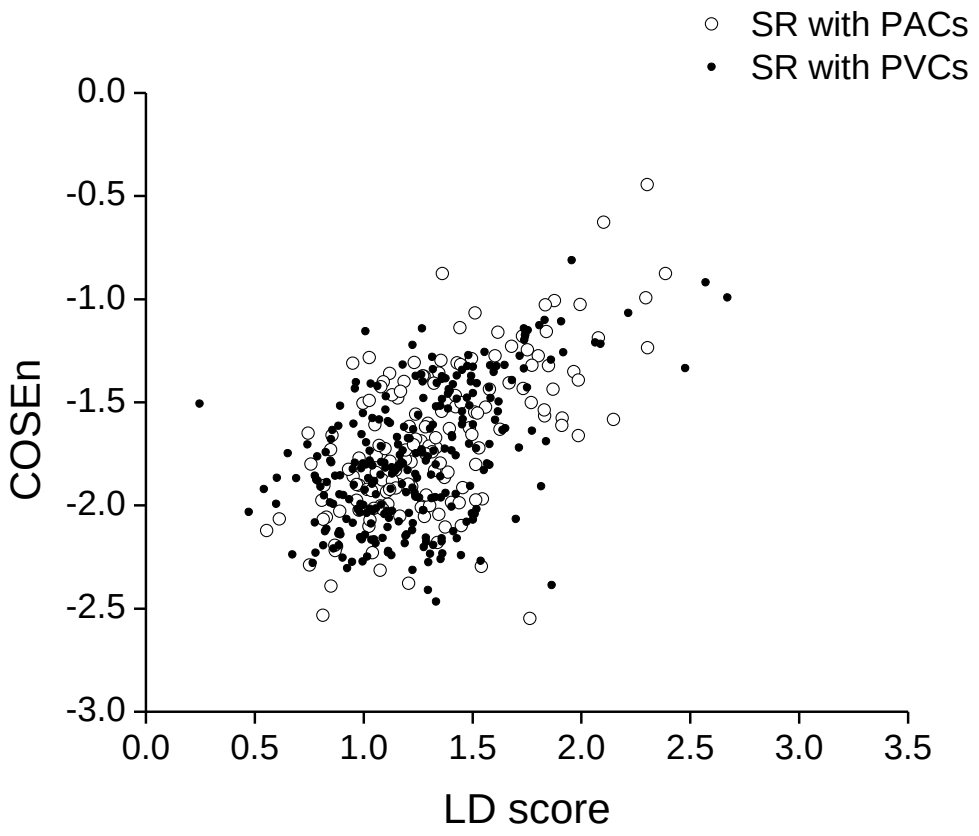

Figure 3.4 COSEn and LD score values for SR with PVCs represented with circle and SR with PACs represented with cross. Notice the overlap between the two groups.

Moreover, we also do not find any difference in the mortality rate related with the two classes. This is surprising, since it is documented the greater association of PVCs with a rising in the risk of cardiac morbidity and mortality, as discussed in §3.1, while PACs are considered harbinger of AF, but not important risk factors for death per se.

The most important finding is the greatly reduced mortality risk in the patients with the lowest values of both the dynamical measures. However, a blue region is also observable in the upper right corner, where the AF patients place. This is related to limit number of patients and high percentage of survivors as depicted in Figure 3.2. When computing the ratio between the joint distributions of the people who died and the whole population, this situation generates a low risk region which is not consistent with the value of risk of the rest of AF patients.

Heart rate dynamics, alone, can inform on the mortality risk. Condition characterized by AF, high burden of ectopy and reduced variability are confirmed to be associated with mortality in ambulatory population.

Chapter 4

Discussion and Conclusion

4.1 Cardiac rhythm classification from RR intervals

We tackled the problem of arrhythmia detection and classification based on RR interval time series using linear and dynamical measures to discriminate among NSR, AF and SR with ectopy. The RR interval time series of 24hr ECG recordings from 2'722 ambulatory patients were divided into 10-minute segments, we measured three different indices: the Coefficient of Sample Entropy, the scaling exponent using Detrended Fluctuation Analysis, and the Local Dynamics score. We tested the hypothesis that these measures, added to standard measures of heart rate and heart rate variability, can improve the classification performance. Our major finding is the improvement in the distinction of SR with ectopy using the dynamical measures from the other two groups. The positive predictive value using either regression models or *k*-NN analysis was 85%, with higher values for the diagnosis of NSR (96%) and AF (90%). The threshold to classify a segment as SR with ectopy rather than NSR, was fixed to be 10% of ectopy burden – this reflects clinical practice, and accuracy increased further if the threshold for diagnosing ectopy was higher.

The models were internally validated using 10-fold cross-validation and externally validated by using the canonical MIT-BIH databases of NSR, AF and other arrhythmias (ARH). In this latter case, the positive predictive values for NSR and AF rose to 99% and 96%, respectively, but fell for SR with ectopy to 45%. This may be explained by the much lower incidence of SR with ectopy in the highly selected MIT-BIH databases, where they represented <1% of the 11'196 10-minute segments, compared with 13% of the 377'825 10-minute segments in the UVa database.

Surprisingly, these measures do not distinguish well between atrial and ventricular premature beats, a potentially important clinical distinction. Atrial

premature beats may be harbingers of AF, and ventricular premature beats are associated with increased mortality, especially when structural heart disease is present.

4.2 Mortality risk evaluation

We evaluated the incidence of deaths in the UVa Holter population using two specific indices of HR dynamics, COSEn and LDs. A low-risk region with a prevalence of patients in NSR, is characterized by low values of both, implying SR without a high burden of ectopy. Situations related to higher risk are SR with reduced HRV, SR with an increasing amount of ectopy and AF.

The important finding is that there is a great increase in the risk of mortality related only to the cardiac rhythm of the patients. As already discussed in chapter 1, many studies in literature assessed AF as an independent risk factor for stroke and for increased morbidity and mortality. Situations with high burden of ectopic beats precede AF and lead to poor prognosis per se. Reduced heart rate variability is a sign of loss of capacity of the organism to adapt to the ever-changing environments, manifesting a dangerous situation of disease.

The mortality risk color map can be a very effective way for clinicians to assess the risk of patients associated with the presence of arrhythmias, thanks to its simplicity and easiness of understanding.

4.2 Clinical implications

The clinical importance of accurate detection of AF is related to the specific treatments that the presence of the arrhythmia requires. For example, the distinction between AF and SR with ectopy can be difficult without PQRST waveforms, but is nonetheless important for two reasons. First, the diagnosis of AF calls for decisions about anticoagulation and for the monitoring process of the patient, such as prescription of diagnostic ECG. Second, atrial ectopy may anticipate AF, and ventricular ectopy may lead to cardiomyopathy or in other ways increase the risk of mortality (Lee et al. 2012). An atrial ectopy burden of even less than 1% increases

the risk of AF over the next 5 to 15 years (Dewland et al, 2013). More than 10% ventricular ectopy can be associated with left ventricular dysfunction and clinical heart failure syndromes that are reversed by ablation of the ectopic site (Lee et al, 2012) (Yokokawa et al, 2013) (Baman et al, 2010).

An accurate arrhythmias detection and classification together with an effective method to determine the risk of the subject associated with that specific arrhythmia, both based only on RR interval time series, could have an important clinical impact for the management of hospitalized and ambulatory outpatients.

4.3 Limitations

Our clinical emphasis constrains our analysis in several ways. First, we consider atrial flutter to be the same as AF. This approach, which is based on the similarities in clinical management, can certain lead to misclassifications. The dynamics of atrial flutter when AV conduction is fixed can never be considered the same as AF. The regularity with which AFL rhythm can appear is responsible for most of the 9 to 10% misclassification error of AF as NSR.

Second, we assigned the diagnosis of AF when as little as 30 seconds, or 5% of a 10-minute segment was present. This is consistent with clinical practice, where episodes lasting as in our case elicit full consideration in AHA guidelines (Fuster et al, 2006), and thus can lead to treatment measures as for AF.

Finally, as previously stated, we assigned the diagnosis of ectopy when as little as 10% is present. The end result of these classification produced a diagnose of AF or SR with ectopy even when the rhythm is 90% or more purely normal SR.

4.4 Future developments and applications

The analyses were performed using an average of the values of COSEn and LDs estimated over 10 minute epochs. The potentiality of this approach consists in having an update of these indices every 30 seconds, so this type of analysis can be performed in a clinical setting such as in Intensive Care Unit where a continuous

monitoring of the changes in cardiac rhythm and their relative risk is crucially important and can be life-saving.

The idea of a "risk map" where regions of low, average and high mortality risk are depicted, can find interesting applications in clinical care too. The map permits to follow the patient course and to see if the therapy is able to maintain the patient or to bring the patient back to the safe region. The monitoring could be performed also real time.

An example of the effectiveness of the classifier in a real time context is reported in Figure 4.1. The RR interval time series is depicted with dots, the line at the bottom represents the output of the classification model proposed in this thesis with an update performed every two minutes. In panels (*a*) and (*b*) are presented two cases of 24-hour recordings of two different patients of the UVa Holter database. The first presents an episode of AF about 3 hour long, while the second has a very high burden of atrial premature beats all over the duration of the Holter registration and a single episode of NSR of about 3 hours. A zoom of the transition from one rhythm to the other is shown in panels (*c*) and (*d*), respectively. The transition from NSR to AF (panel (*c*)) is preceded by 10 minutes of SR with ectopy, as the model output precisely tracks.

Moreover, the potentialities of an automatic RR-based arrhythmias classifier are enormously important in new growing fields as home care monitoring and telemedicine, where it could find extensive applications. Some of the important challenges in western countries society are represented by the growth in the aging population, the changes in lifestyle, the need for healthcare cost containment and the need for improvement and monitoring of healthcare quality. It is clear how cardiac abnormalities and risk monitoring plays a central role in this scenario. Telemedicine has been extensively investigated and today it can contribute to new trends in healthcare system through all-day monitoring of vital signs without the commitment of hospital personnel or hospital facilities.

Finally, this work proved the benefit of dynamical measures in the problem of arrhythmias detection and classification. COSEn and LDs were already tested as efficient measures to specifically detect AF and abnormal local dynamics, respectively (Lake and Moorman, 2011) (Moss et al, 2014). However, this work

included the short-term scaling exponent obtained from DFA computed over 10 minute segments as a useful parameter to distinguish three very important clinical arrhythmias, such as NSR, AF and SR with a certain burden of ectopy. In the work of Yeh et al (2009) they proposed the same calculation of the short-term scaling exponent over 10 minutes with a maximum box size of 11 beats, but the goal of the study was to discriminate healthy patients from patients with congestive heart failure. However, future improvements can be done by investigating different types of classification algorithms, as many works demonstrated the efficiency of Neural Networks, Support Vector Machine or Fuzzy logic in the classification problem (Acharya et al, Comprehensive analysis of cardiac health using heart rate signals, 2004) (Bardossy et al, 2013) (Mohammadzadeh Asl et al, 2008).

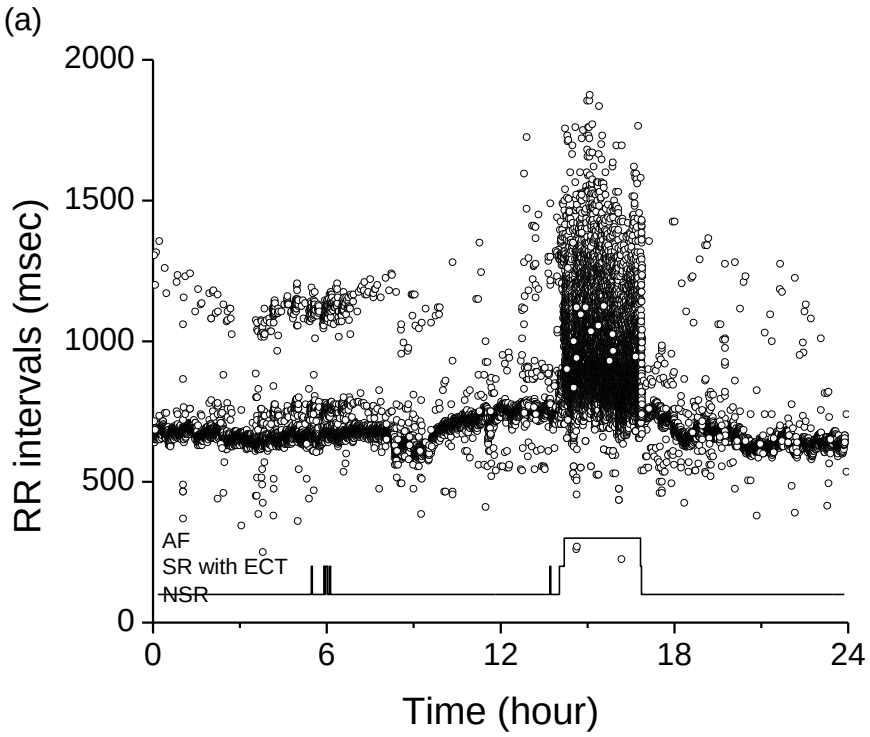
(a)
RR intervals (msec)
2000
1500
1000
500
0
AF
SR with ECT
NSR
0
6
12
18
24
Time (hour)

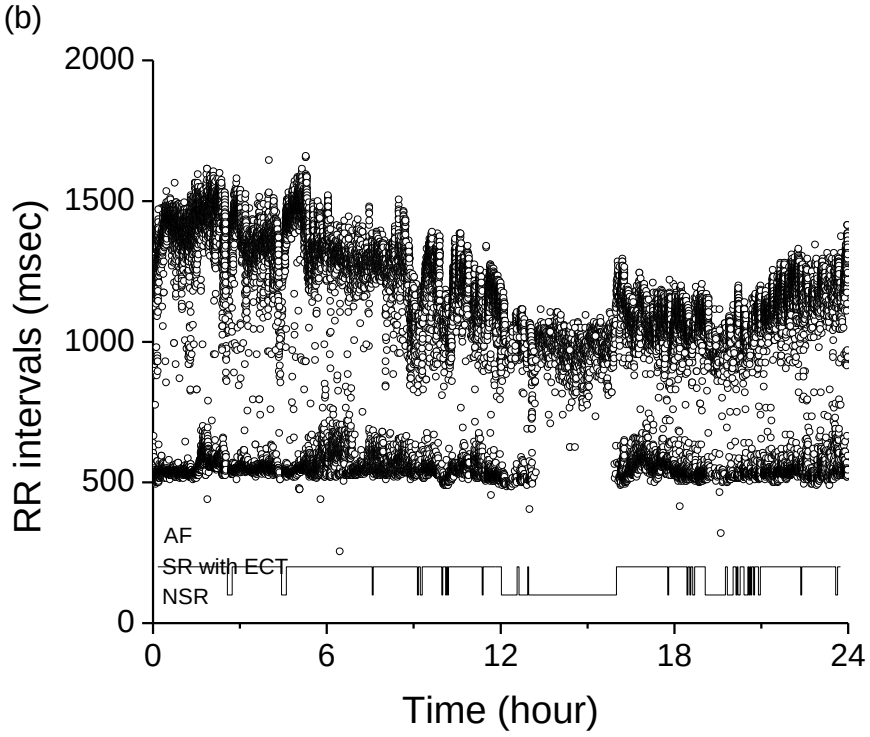
(b)
RR intervals (msec)
2000
1500
1000
500
0
AF
SR with ECT
NSR
0
6
12
18
24
Time (hour)

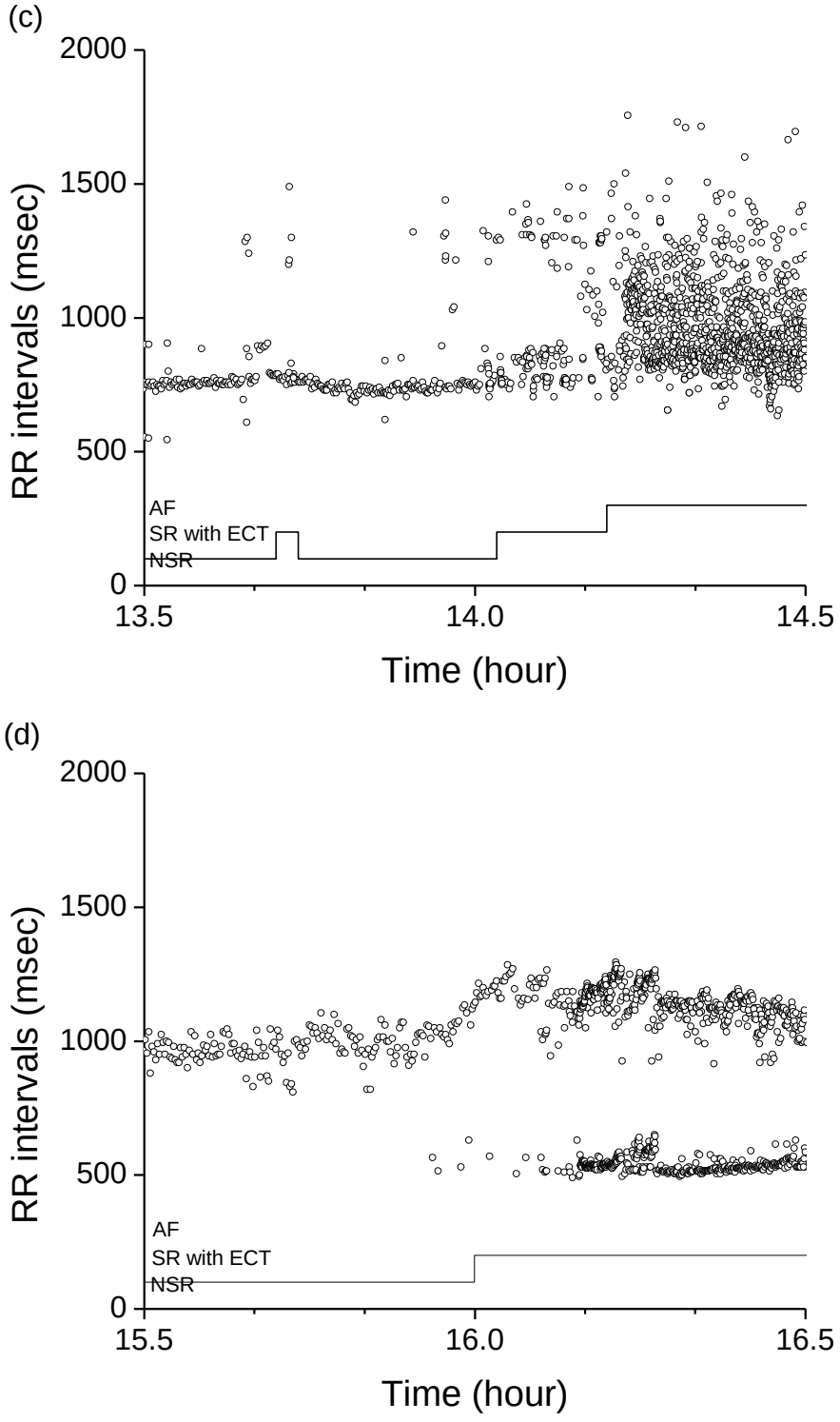

Figure 4.1 In the panels (*a*) and (*b*) there are two examples of 24-hour recordings from two distinct patients of the UVa Holter database. In (*a*) an AF episode occurs after about 14 hours and sparsely episodes of ectopic beats are present; in (*b*) the rhythm is dominated by atrial premature contractions, unless a 4-hour periods of NSR. The lower solid line indicates the output of the classifier proposed in this work with an update every 2 minutes. In panels (c) and (d) a zoom of the previous signals is presented: in (*c*) the transition from NSR to AF, preceded by episodes of atrial ectopies; in (*d*) the transition from NSR to SR with PACs.

Bibliography

Acharya et al. (2002). Classification of heart rate data using artificial neural network and fuzzy equivalence relation. *Pattern Recognition*, 36:61-68.

Acharya et al. (2003). Classification of cardiac abnormalities using heart rate signals. *Med. Biol. Eng. Comput.*, 42, 288-293.

Acharya et al. (2004). Comprehensive analysis of cardiac health using heart rate signals. *Physiol. Meas.*, 25, 1139-1151.

Acharya et al. (2006). Heart rate variability: a review. *Med Bio Eng Comput*, 44:1031–1051.

Acharya et al. (2008). Automatic identification of cardiac health using modeling techniques: a comparative study. *Information sciences*, 178, 4571-4582.

Anuradha and Reddy. (2005-2008). Cardiac arrhythmia classification using fuzzy classifiers. *Journal of Theoretical and Applied Information Technology* .

Arrigo et al. (2013). Management of Atrial Fibrillation in Critically Ill Patients. *Critical Care Research and Practice* , Article ID 840615, 10 pages .

Baman et al. (2010). Relationship between burden of premature ventricular complexes and left ventricular function. *Heart Rhythm*, 7(7): 865-869.

Bardossy et al. (2013). Fuzzy-logic based diagnostic algorithm for implantable cardioverter defibrillator. *Artificial Intelligence in Medicine*, 60, 113-121.

Barret et al. (2014). Comparison of 24-hour Holter Monitoring with 14-day Novel Adhesive Patch Electrocardiographic Monitoring. *The American Journal of Mediciine*, 127,95.e11-95.e17.

Benjamin et al. (1998). Impact of Atrial Fibrillation on the Risk of Death: The Framingham Heart Study. *Circulation*, 98:946-952.

Botev et al. (2010). Kernel density estimation via diffusion. *The Annals of Statistics*, 38:No.5,2916-2957.

Braun et al. (1998). Demonstration of nonlinear components in heart rate variability of healthy persons. *The American Physiological Society*, 0363-613598.

Bravi et al. (2011). Review and classification of variability analysis techniques with clinical applications. *BioMedical Engineering OnLine*, 10:90.

Buchman et al. (2002). Heart rate variability in critical illness and critical care . *Current Opinion in Critical Care*, 8:311–315.

Cerutti et al. (2007). Long-term invariant parameters obtained from 24-hour Holter recordings: A comparison between different analysis techniques. *CHAOS* , 17, 015108.

Cha et al. (2012). Premature Ventricular Contraction-Induced Cardiomyopathy: A Treatable Condition. *Circ Arrhythm Electrophysiol.*, 5:229-236Circ .

Chazal and Reilly. (2004). Automatic Classification of Heartbeats Using ECG Morphology and Heartbeat Interval Features. *IEEE Transaction on biomedical engineering*, Vol. 51, No. 7.

Cheng and Chan. (1998). Classification of Electrocardiogram using Hidden Markov Models. *IEEE Engineering in Medicine and Biology Society*, Vol 20, No 1.

Chugh et al. (2008). Epidemiology of sudden cardiac death: clinical and reserach implications. *Progress in Cardiovascular Diseases*, Vol.51, No 3, pp 213-228.

Cottrell. (2012). Atrial fibrillation part 1: pathophysiology. *Practice Nursing*, Vol 23, No 1.

DeMazumder et al. (2013). Dynamic Analysis of Cardiac Rhythms for Discriminating Atrial Fibrillation From Lethal Ventricular Arrhythmias. *Circ Arrhythm Electrophysiol.*, 6:555-561.

Dewland et al. (2013). Atrial ectopy as a predictor of incident atrial fibrillation: a cohort study. *Ann Intern Med* , 159(11): 721-728.

Eckmann and Ruelle. (1985). Ergodic theory of chaos and strange attractors. *Rev Mod Phys*, 57: 617-654.

Ferrario et al. (2006). Comparison of Entropy-Based Regularity Estimators: Application to the Fetal Heart Rate Signal for the Identification of Fetal Distress. *IEEE Transaction on biomedical engineering*, Vol. 53, No. 1.

Fuster et al. (2006). ACC/AHA/ESC 2006 Guidelines for the Management of Patients with Atrial Fibrillation: a report of the American College of Cardiology/American Heart Association Task Force on Practice Guidelines and the European Society of Cardiology Committee for Practice. *Circulation*, 114(7): e257-e354.

Go et al. (2013). Heart Disease and Stroke Statistics—2013 Update. A Report From the American Heart Association. *Circulation*, 127:e6-e245.

Golberger et al. (1985). On a Mechanism of Cardiac Electrical Stability: The Fractal Hypothesis. *Biophysical Journal*, Volume 48.

Goldberger. (1996). Non-linear dynamics for cliicians: chaos theory,fractals and complexity at the bedside. *the Lancet*, 347;1312-1314.

Goldberger et al. (2000). PhysioBank, PhysioToolkit, and PhysioNet: Components of a New Research Resource for Complex Physiologic Signals. *Circulation*, 101(23):e215-e220.

Grassberger and Procaccia. (1983). Estimation of the Kolmogorov entropy from a chaotic signal. *Phys Rev A*, 28: 2591-2593.

Haissaguerre et al. (1998). Spontaneous initiation of atrila fibrillation by ectopic beats originating in the pulmonary veins. *N Engl J Med*, 339:659-66.

Hart et al. (2007). Meta-analysis: Antithrombotic Therapy to Prevent Stroke in Patients Who Have Nonvalvular Atrial Fibrillation. *Ann Intern Med.* , 146:857-867.

Healy et al. (2012). Subclinical Atrial Fibrillation and the Risk of Stroke. *N Engl J Med*, 366:120-9.

Hindricks et al. (2010). Performance of a New Leadless Implantable Cardiac Monitor in Detecting and Quantifying Atrial Fibrillation Results of the XPECT Trial. *Circ Arrhythm Electrophysiol*, 3:141-147.

Hoffman et al. (2002). The Incidence of Arrhythmias in a Pediatric Cardiac Intensive Care Unit. *Pediatr. Cardiol*, 23:598-604.

Hosseini et al. (2006). The comparison of different feed forward neural network architectures for ECG signal diagnosis. *Medical Engineering and Physics*, 28, 372-378.

Huang et al. (2011). A Novel Method for Detection of the Transition Between Atrial Fibrillation and Sinus Rhythm. *IEEE Transaction on biomedical engineering*, VOL. 58, NO. 4.

Kamath. (2012). A Novel approach to arrhythmias classification using RR interval and Teager energy. *Journal of Engineering Science and Technology* , Vol. 7, No. 6, 744 - 755.

Kannel et al. (1998). Prevalence, Incidence, Prognosis, and Predisposing Conditions for Atrial Fibrillation: Population-Based Estimates. *Am J Cardiol* , 82:2N–9N.

Kastor. (2002). Cardiac Arrhythmias. *Encyclopedia of life sciences*.

Khoo and Lip. (2009). Acute Management of Atrial Fibrillation. *CHEST*, 135:849–859.

Knotzer et al. (2000). Tachyarrhythmias in a Surgical Intensive Care Unit: a case control epidemiologic study. *Intensive Care Med*, 26:908-914.

Kolmogorov. (1958). New metric invariant of transitive dynamical systmen and endomorphisms of Lebesgue spaces. *Doklady Rus Acad Sci*, 119: 861-864.

Kolmogorov. (1959). Entropy per unit time as a metric invariant of automorphism. *Doklady Rus Acad Sci*, 124: 754-755.

Krahn et al. (1995). The Natural History of Atria1 Fibrillation: Incidence, Risk Factors, and Prognosis in the Manitoba Follow-Up Study . *The american journal of medicine*, Vol. 98.

Lake. (2006). Renyi entropy measures of heart rate Gaussianity. *IEEE Trans Biomed Eng*, 53: 21–27.

Lake. (2009). Nonparametric entropy estimation using kernel density. *Methods Enzymol*, 467:531-46.

Lake and Moorman. (2011). Accurate estimation of entropy in very short physiological time series: the problem of atrial fibrillation detection in implanted ventricular devices. *Am J Physiol Heart Circ Physiol*, 300:H319-H325.

Lee et al. (2012). The prognostic significance of premature ventricular complexes in adults without clinically apparent heart disease: a meta-analysis and systematic review. *Heart*, 98:1290-1298.

Leong et al. (2013). Atrial fibrillation is associated with increased mortality: causation or association? *European Heart Journal*, 34, 1027–1030 .

Levine et al. (2001). Hemorrhagic Complications of Anticoagulant Treatment. *CHEST*, 119:108S–121S.

Lian et al. (2011). A simple method to detect atrial fibrillatio using RR intervals. *Am J Cardiol*, 107:1494-1497.

Minami et al. (1999). Real-Time Discrimination of Ventricular Tachyarrhythmia with Fourier-Transform Neural Network. *IEEE Transaction on biomedical engineering*, VOL. 46, NO. 2.

Mohammadzadeh Asl et al. (2008). Support vector machine-based arrhythmia classification using reduced features of heart rate variability signal. *Artificial Intelligence in Medicine*, 44, 51-64.

Moody and Mark. (1990). QRS morphology representation and noise estimation using the Karhunen-Loeve transform. *IEEE*, 0276-6574/90/0000/0269.

Moss et al. (1979). Ventricular ectopic beats and their relation to sudden and nonsudden cardiac death after myocardial infarction. *Circulation*, 60:998-1003.

Moss et al. (2014). Local dynamics of heart rate: detection and prognostic implications. *Physiological Measurement*, In press.

Ofoma et al. (2012). Premature Cardiac Contractions and Risk of Incident Ischemic Stroke. *J Am Heart Assoc.*, 1:e002519.

Ouelli et al. (2012). AR Modeling for Automatic Cardiac Arrhythmia Diagnosis using QDF Based Algorithm. *International Journal of Advanced Research in Computer Science and Software Engineering*, Vol 2, Issue 5, pp 493-499.

Owis et al. (2002). Study of Features Based on Nonlinear Dynamical Modeling in ECG Arrhythmia Detection and Classification. *IEEE Transaction on biomedical engineering*, Vol. 49, No. 7.

Pena et al. (2009). Applying fractal analysis to short sets of heart rate variability data. *Med Biol Eng Comput*, 47(7): 709-717.

Peng et al. (1995). Quantification of scaling exponents and crossover phenomena in nonstationary heartbeat time series. *CHAOS*, Vol. 5, No. 1.

Pincus. (1991). Approximate entropy as a measure of system complexity. *Proc Natl Acad Sci USA* , 88: 2297–2301.

Prystowsk. (2000). Management of Atrial Fibrillation: Therapeutic Options and Clinical Decisions. *Am J Cardiol*, 85:3D–11D.

Reinelt et al. (2001). Incidence and type of cardiac arrhythmias in critically ill patients: a single center experience in a medical-cardiological ICU. *Intensive Care Med*, 27:1466-1473.

Ricci et al. (2009). Remote control of implanted devices through Home Monitoring technology improves detection and clinical management of atrial fibrillation. *European society of cardiology*, 11, 54–61.

Richman and Moorman. (2000). Physiological time series analysis using approximate entropy and sample entropy. *Am J Phisiol Heart Circ Physiol*, 278: H2039-H2049.

Ruberman et al. (1981). Ventricular premature complexes and sudden death after myocardial infarction. *Circulation*, 64:297-305.

Sarkar et al. (2008). A Detector for a Chronic Implantable Atrial Tachyarrhythmia Monitor. *IEEE Transaction on biomedical engineering*, Vol. 55, No. 3.

Senhadij et al. (1995). Comparing Wavelet transtorms for Recognizing Cardiac Patterns. *IEEE engineering in medicine and biology*, 0739-51 75.

Shannon. (1948). A Mathematical Theory of Communication. *The Bell System Technical Journal*, Vol. 27, pp. 379–423, 623–656.

Shieh et al. (2006). Detrended fluctuation analyses of short-term heart rate variability in surgical intensive care units. *Biomed Eng Appl Basis Comm*, 18: 67-72.

Sinai. (1959). On the notion of entropy of a dynamical system. *Doklady Rus Acad Sci*, 124: 768-771.

Song et al. (2005). Support Vector Machine Based Arrhythmia Classification Using Reduced Features. *International Journal of Control Automation and Systems*, vol. 3, no. 4, pp. 571-579.

Southall et al. (1982). Prolonged Apnea and Cardiac Arrhythmias in Infants Discharged from Neonatal Intensive Care Units: Failure to Predict an Increased Risk for Sudden Infant Death Syndrome. *Pediatrics*, 70;844.

Stewart et al. (2002). A Population-Based Study of the Long-term Risks Associated with Atrial Fibrillation:20-Year Follow-up of the Renfrew/Paisley Study. *Am J Med.* , 113:359–364.

Tateno and Glass. (2001). Automatic detection of atrial fibrillation using the coefficient of variation and density histograms of RR and ΔRR intervals. *Med. Biol. Eng. Comput.*, 39, 664-671.

Tompkins. (1995). Detecting Ventricular Fibrillation. Selecting the appropriate time-frequency analysis tool for the application. *IEEE engineering in medicine and biology*, 0739-51 75.

Tsipouras and Fotiadis. (2003). Automatic arrhythmia detection based on time and time-frequency analysis of heart rate variability. *Computer Methods and Programs in Biomedicine*, 74,95-108.

Tsipouras et al. (2004). An arrhythmia classification system based on the RR-interval signal. *Artificial Intelligence in Medicine*, 33, 237—250.

Wallmann et al. (2007). Frequent Atrial Premature Beats Predict Paroxysmal Atrial fibrillation in stroke patients. *Stroke*, 38:2292-2294.

Wang et al. (2001). A Short-Time Multifractal Approach for Arrhythmia Detection Based on Fuzzy Neural Network. *IEEE Transaction on biomedical engineering*, Vol. 48, No. 9.

Wolf et al. (1991). Atrial fibrillation as an independent risk factor for stroke: the Framingham Study. *Stroke*, 22:983-988.

Xiao et al. (2010). Nearest neighbor and logistic regression analyses of clinical and heart rate characteristics in the early diagnosis of neonatal sepsis. *Med Decis Making*, 30(2): 258–266.

Yaghouby et al. (2009). Classification of Cardiac Abnormalities Using Reduced Features of Heart Rate Variability Signal. *World Applied Sciences Journal*, 6 (11): 1547-1554.

Yeh et al. (2009). Parameter Investigation of Detrended Fluctuation Analysis for Short-term Human Heart Rate Variability. *Journal of Medical and Biological Engineering*, 30(5): 277-282.

Yokokawa et al. (2013). Recovery from left ventricular dysfunction after ablation of frequent premature ventricular complexes. *Heart Rhythm*, 10:172-175.

Yu and Chen. (2008). Electrocardiogram beat classification based on wavelet transformation and probabilistic neural network. *Pattern Recognition Letters*, 1142–1150.